HAL
open science

Guaranteed and robust a posteriori bounds for Laplace eigenvalues and eigenvectors: a unified framework

Eric Cancès, Geneviève Dusson, Yvon Maday, Benjamin Stamm, Martin Vohralík

To cite this version:

Eric Cancès, Geneviève Dusson, Yvon Maday, Benjamin Stamm, Martin Vohralík. Guaranteed and robust a posteriori bounds for Laplace eigenvalues and eigenvectors: a unified framework. Numerische Mathematik, 2018, 140 (4), pp.1033-1079. 10.1007/s00211-018-0984-0 . hal-01483461v3

HAL Id: hal-01483461

https://inria.hal.science/hal-01483461v3

Submitted on 12 Jul 2018

HAL is a multi-disciplinary open access archive for the deposit and dissemination of scientific research documents, whether they are published or not. The documents may come from teaching and research institutions in France or abroad, or from public or private research centers.

L'archive ouverte pluridisciplinaire **HAL**, est destinée au dépôt et à la diffusion de documents scientifiques de niveau recherche, publiés ou non, émanant des établissements d'enseignement et de recherche français ou étrangers, des laboratoires publics ou privés.

Guaranteed and robust a posteriori bounds for Laplace eigenvalues and eigenvectors: a unified framework*

Eric Cancès[**¶] Geneviève Dusson[††] Yvon Maday[†‡‖] Benjamin Stamm[§‡‡]
Martin Vohralík[¶**]

July 12, 2018

Abstract

This paper develops a general framework for a posteriori error estimates in numerical approximations of the Laplace eigenvalue problem, applicable to all standard numerical methods. Guaranteed and computable upper and lower bounds on an arbitrary simple eigenvalue are given, as well as on the energy error in the approximation of the associated eigenvector. The bounds are valid under the sole condition that the approximate i-th eigenvalue lies between the exact $(i-1)$-th and $(i+1)$-th eigenvalue, where the relative gaps are sufficiently large. We give a practical way how to check this; the accuracy of the resulting estimates depends on these relative gaps. Our bounds feature no unknown (solution-, regularity-, or polynomial-degree-dependent) constant, are optimally convergent (efficient), and polynomial-degree robust. Under a further explicit, a posteriori, minimal resolution condition, the multiplicative constant in our estimates can be reduced by a fixed factor; moreover, when an elliptic regularity assumption on the corresponding source problem is satisfied with known constants, this multiplicative constant can be brought to the optimal value of 1 with mesh refinement. Applications of our framework to nonconforming, discontinuous Galerkin, and mixed finite element approximations of arbitrary polynomial degree are provided, along with numerical illustrations. Our key ingredient are equivalences between the i-th eigenvalue error, the associated eigenvector energy error, and the dual norm of the residual. We extend them in an appendix to the generic class of bounded-below self-adjoint operators with compact resolvent.

Key words: Laplace eigenvalue problem, a posteriori estimate, guaranteed eigenvalue bound, guaranteed eigenvector error bound, abstract framework, nonconforming finite element method, discontinuous Galerkin method, mixed finite element method

1 Introduction

Precise numerical approximation of eigenvalues and eigenvectors of elliptic operators on general domains is crucial in countless applications. In addition to standard conforming Galerkin (variational) approximations,

**Université Paris-Est, CERMICS, Ecole des Ponts, 6 & 8 Av. Pascal, 77455 Marne-la-Vallée, France. (cances@cermics.enpc.fr).

¶Inria, 2 rue Simone Iff, 75589 Paris, France (martin.vohralik@inria.fr).

††Mathematics Institute, University of Warwick, Coventry CV47AL, United Kingdom (g.dusson@warwick.ac.uk).

†Sorbonne Université, Université Paris-Diderot SPC, CNRS, Laboratoire Jacques-Louis Lions, LJLL, F-75005 Paris (maday@ann.jussieu.fr).

‡Institut Universitaire de France, 75005, Paris, France.

‖Division of Applied Mathematics, Brown University, 182 George St, Providence, RI 02912, USA.

§Center for Computational Engineering Science, RWTH Aachen University, Aachen, Germany (stamm@mathcces.rwth-aachen.de).

‡‡Computational Biomedicine, Institute for Advanced Simulation IAS-5 and Institute of Neuroscience and Medicine INM-9, Forschungszentrum Jülich, Germany.

*This work was supported by the ANR project MANIF "Mathematical and numerical issues in first-principle molecular simulation". Part of this work has been supported from French state funds managed by the CalSimLab LABEX and the ANR within the Investissements dAvenir program (reference ANR-11-LABX-0037-01). The last author has also received funding from the European Research Council (ERC) under the European Union's Horizon 2020 research and innovation program (grant agreement No 647134 GATIPOR).

nonconforming methods such as nonconforming finite elements, discontinuous Galerkin elements, or mixed finite elements are very popular, and one naturally asks the question of the size of the error in their eigenvalue and eigenvector approximations.

The issue of error control is usually tackled via the a posteriori estimates theory. Recently, powerful estimates were obtained for nonconforming approximations of the Laplace source problem, see Destuynder and Métivet [29], Ainsworth [1, 2], Kim [48, 49], Vohralík [62], Carstensen and Merdon [22], or Ern *et al.* [35, 37, 38], see also the references therein. The Laplace eigenvalue problem seems to be structurally more difficult. Recently, though, *guaranteed* a posteriori estimates on the error in the *i-th eigenvalue* have been obtained in Carstensen and Gedicke [20] and Liu [51]. The theory of [20, 51] applies for arbitrarily coarse meshes and gives convincing numerical results in many test cases. One could, however, comment that these results only seem to apply to the lowest-order nonconforming finite element method, the arguments used are of a priori nature that relies on an interpolation estimate, and an overestimation in presence of singularities and graded meshes may appear as the bounds feature the diameter of the largest mesh element, see [20, Section 6.3]. More precisely, these bounds loose accuracy if the diameter of the largest mesh element does not tend to zero. Armentano and Durán [6], Luo *et al.* [53], Hu *et al.* [45, 46], or Yang *et al.* [63] also derived (guaranteed) eigenvalue estimates for the nonconforming finite element method, where, however, a saturation assumption may be necessary and/or the results are valid only asymptotically. Errors in both eigenvalue and eigenvector approximations in nonconforming methods have also been studied previously, although rather seldom. We refer in particular to Dari *et al.* [26] for nonconforming finite elements, to Giani and Hall [40] for discontinuous Galerkin elements, and to Durán *et al.* [34] and Jia *et al.* [47] for mixed finite elements. Unfortunately, these estimates systematically contain solution-independent but unknown constants as well as solution-dependent, uncomputable terms, claimed higher order on fine enough meshes via a priori arguments.

The purpose of the present paper is to extend our conforming theory of Cancès *et al.* [17] to a *general framework* for guaranteed and optimally convergent *a posteriori bounds* for both arbitrary simple *i-th eigenvalue* and the associated *eigenvector* of the Laplace eigenvalue problem. Let $\Omega \subset \mathbb{R}^d$, $d = 2, 3$, be a polygonal/polyhedral domain with a Lipschitz boundary. Let the exact eigenvector and eigenvalue pairs (u_i, λ_i) satisfy

$$-\Delta u_i = \lambda_i u_i \quad \text{in } \Omega, \tag{1.1}$$

with the condition $\|u_i\| = 1$, see (2.1) below for the precise weak formulation. We denote by $(\cdot,\cdot)$ the $L^2(\Omega)$ or $[L^2(\Omega)]^d$ scalar product over Ω and by $\|\cdot\|$ the associated norm and let

$$H^1(\mathcal{T}_h) := \{v \in L^2(\Omega);\ v|_K \in H^1(K) \quad \forall K \in \mathcal{T}_h\} \tag{1.2}$$

be the so-called *broken Sobolev space*, where the traces on mesh faces do not need to coincide. It is defined over a computational mesh $\mathcal{T}_h$ of the domain Ω; details of the setting are given in Section 2. On $H^1(\mathcal{T}_h)$, we generalize the usual weak gradient ∇ of $H^1(\Omega)$ to the discrete gradient ∇_θ featuring a parameter $\theta \in \{-1, 0, 1\}$, see (2.5) below. We consider here an abstract setting where the approximate eigenvector–eigenvalue pair (u_{ih}, λ_{ih}) is not necessarily linked to any particular numerical method, $u_{ih} \in H^1(\mathcal{T}_h)$ is a piecewise polynomial possibly nonconforming in the sense that $u_{ih} \notin H^1_0(\Omega)$ and not necessarily scaled to $\|u_{ih}\| = 1$, $\lambda_{ih} \in \mathbb{R}^+$, and the relation $\|\nabla_\theta u_{ih}\|^2 = \lambda_{ih}$ typically does not hold at the discrete level in contrast to the continuous one. Concrete examples of numerical methods fitting to our setting can be found later in Section 7.

Our main tools are an *equilibrated flux reconstruction* $\boldsymbol{\sigma}_{ih} \in \mathbf{H}(\mathrm{div}, \Omega)$ satisfying $\nabla\cdot\boldsymbol{\sigma}_{ih} = \lambda_{ih} u_{ih}$ and an *eigenvector reconstruction* $s_{ih} \in H^1_0(\Omega)$, both defined in Section 3. These are piecewise polynomials such that $-\boldsymbol{\sigma}_{ih}$ and ∇s_{ih} are as close as possible to the discrete gradient $\nabla_\theta u_{ih}$. They are constructed over patches of mesh elements following Destuynder and Métivet [30], Braess and Schöberl [13], Carstensen and Merdon [22], and Ern and Vohralík [38], see also the references therein. We employ them in Section 4 to show in particular how the dual norm of the residual of the pair (s_{ih}, λ_{ih}) can be bounded in a computable way. Section 5 then bounds the $L^2(\Omega)$-norm of the Riesz representation of the residual of (s_{ih}, λ_{ih}) under an assumption of elliptic regularity on the corresponding Laplace source problem. It enables later to give improved computable estimates in the considered nonconforming setting.

Our main results are collected in Section 6 and crucially rely on [17, Section 3], where mutual relations between the i-th eigenvalue error, the associated eigenvector energy error, and the dual norm of the residual in terms of an arbitrary pair $(\tilde{s}_{ih}, \lambda_{ih}) \in H^1_0(\Omega) \times \mathbb{R}^+$ such that $\|\tilde{s}_{ih}\| = 1$ are given. Using $\tilde{s}_{ih} := s_{ih}/\|s_{ih}\|$,

where s_{ih} is the above eigenvector reconstruction, inequality (6.4) of Theorem 6.1 in particular gives

$$\|\nabla \tilde{s}_{ih}\|^2 - \eta_i^2 \le \lambda_i, \tag{1.3a}$$

where η_i is an a posteriori error estimator with a typical structure

$$\eta_i = m_{ih}(\lambda_{ih}\|u_{ih} - s_{ih}\|/\sqrt{\underline{\lambda}_1} + \|\nabla s_{ih} + \boldsymbol{\sigma}_{ih}\|)/\|s_{ih}\|. \tag{1.3b}$$

Thus (1.3a) gives a *guaranteed* and computable lower bound for the i-th exact *eigenvalue* λ_i. An upper bound on λ_i is recalled in inequality (6.14) of Theorem 6.3. A *guaranteed* and computable a posteriori estimate on the associated *eigenvector energy error* is given next, see in particular estimate (6.16) of Theorem 6.4 revealing

$$\|\nabla_\theta(u_i - u_{ih})\| \le \eta_i + \|\nabla_\theta(u_{ih} - \tilde{s}_{ih})\|. \tag{1.3c}$$

The eigenvalue and eigenvector error bounds (1.3) are *efficient* (optimally convergent) in the sense that

$$\begin{aligned} \eta_i + \|\nabla_\theta(u_{ih} - \tilde{s}_{ih})\| \le C_i(&\|\nabla_\theta(u_i - u_{ih})\| + \text{ consistency terms} \\ &+ \text{norm of mean values of jumps of } u_{ih}), \end{aligned} \tag{1.4}$$

see inequality (6.17) of Theorem 6.5. Here C_i is a generic constant that only depends on λ_1, λ_{ih}, on the lower bound $\underline{\lambda}_{i+1}$ of λ_{i+1}, possibly on the upper bound $\overline{\lambda}_{i-1}$ of λ_{i-1}, on the shape of Ω, and on some (broken) Poincaré–Friedrichs constants over patches of elements and a stability constant of mixed finite elements (both only depending on the shape regularity of the mesh and on the space dimension d). The constant C_i is in particular independent of the polynomial degree of u_{ih}, leading to *polynomial-degree robustness*. The consistency terms above may not be present, typically for nonconforming finite elements. Similarly, the jump mean values of u_{ih} are zero in nonconforming and mixed finite elements, and this term also vanishes in our developments for the symmetric variant of the discontinuous Galerkin finite element method when the parameter θ equals 1.

The above results are valid under the condition (6.1), requesting λ_{ih} to lie between computable bounds $\underline{\lambda}_{i+1}$ and $\overline{\lambda}_{i-1}$ (when $i > 1$) on the surrounding exact eigenvalues λ_{i+1} and λ_{i-1}, see the discussion in [17, Remark 5.4] for its practical verification. We also need the residual orthogonality condition of Assumption 3.1 in order to reconstruct the equilibrated flux. Then, for u_{ih} a piecewise polynomial of degree p, the reconstructions s_{ih} and $\boldsymbol{\sigma}_{ih}$ are prescribed in discrete spaces of order $p+1$. There is no specific condition on the fineness of the mesh in Case A of Theorems 6.1 and 6.4, but the multiplicative factor m_{ih} in (1.3b) contains the relative gap of the form $\max\{(\frac{\lambda_{ih}}{\overline{\lambda}_{i-1}} - 1)^{-1}, (1 - \frac{\lambda_{ih}}{\underline{\lambda}_{i+1}})^{-1}\}$. Two improvements are possible. Under the computable minimal resolution criterion (6.6b) (satisfied for fine enough meshes), m_{ih} is reduced by a fixed factor, see Case B of Theorems 6.1 and 6.4. If an elliptic regularity assumption on the corresponding source problem is satisfied and if the minimal resolution condition (6.8b) holds, the relative gap in m_{ih} is multiplied by a power of the mesh size h, so that m_{ih} can be brought to the optimal value of 1 in the limit of mesh size tending to zero, at least for nonconforming, mixed, and symmetric discontinuous Galerkin methods, which we show in Case C of Theorems 6.1 and 6.4. The efficiency constant C_i from (1.4) or (6.17) can be fully traced from the detailed estimates of Theorem 6.5; in particular it deteriorates for increasing eigenvalues.

The application of our abstract results to a given numerical method merely requires the verification of the setting and of Assumption 3.1. We undertake this in Section 7 for nonconforming finite elements, discontinuous Galerkin elements, and mixed finite elements of arbitrary polynomial degree. For mixed finite elements, elementwise postprocessings of the approximate eigenvector and of its flux need to be performed first. Numerical experiments are presented in Section 8 for the nonconforming and discontinuous Galerkin methods and fully support our theoretical findings for a couple of model problems. In particular, the a posteriori applicability conditions (6.6b) and (6.8b) for cases B and C are satisfied here already on very coarse meshes. Some concluding remarks and an outlook are given in Section 9. In particular, inexact algebraic eigenvalue solvers promoted in Mehrmann and Miedlar [55] or Carstensen and Gedicke [20] can be treated as in [17] and the references therein, allowing to generalize the present estimates to an arbitrary iterative solver step where Assumption 3.1 typically does not hold.

We finish our paper by two extensions. We first show in Appendix A that the key relations between the i-th eigenvalue error, the associated eigenvector energy error, and the dual norm of the residual, when u_{ih} is conforming, i.e., $u_{ih} \in H_0^1(\Omega)$, are in fact not restricted to the Laplace operator; we extend them to

the generic class of bounded-below self-adjoint operators with compact resolvent in Theorems A.1 and A.2. Appendix B then gives a further possible improvement of the first eigenvalue upper bound: from $\lambda_1 \leq \|\nabla \tilde{s}_{1h}\|^2$ of (6.15) in Theorem 6.3 to $\lambda_1 \leq \|\nabla \tilde{s}_{1h}\|^2 - \tilde{\eta}_1$ of Proposition B.3.

We only treat here simple eigenvalues and associated eigenvectors; clustered and multiple eigenvalues are dealt with in contribution [18] that we are now finalizing. We rely there on the framework of density matrices and actually provide guaranteed bounds for an arbitrary set of eigenvalues under the sole condition that there is a sufficient gap between this set and the surrounding eigenvalues. This analysis is done in the abstract framework of Appendix A.

2 Setting

Let $H^1(\Omega)$ be the Sobolev space of $L^2(\Omega)$ functions with weak gradients ∇ in $[L^2(\Omega)]^d$. We denote henceforth by $V := H^1_0(\Omega)$ its zero-trace subspace. Later, we will also employ the space $\mathbf{H}(\mathrm{div}, \Omega)$ of $[L^2(\Omega)]^d$ functions with weak divergences $\nabla\cdot$ in $L^2(\Omega)$.

2.1 The Laplace eigenvalue problem

The weak formulation of (1.1) looks for $(u_i, \lambda_i) \in V \times \mathbb{R}^+$ with $\|u_i\| = 1$ and

$$(\nabla u_i, \nabla v) = \lambda_i (u_i, v) \qquad \forall v \in V. \tag{2.1}$$

It is well-known (see, e.g., Babuška and Osborn [8] or Boffi [10] and the references therein) that u_i, $i \geq 1$, form a countable orthonormal basis of $L^2(\Omega)$ consisting of eigenvectors from V; we assume that the sequence of eigenvalues is such that $0 < \lambda_1 < \lambda_2 \leq \ldots \leq \lambda_i \to \infty$. We will actually suppose that the eigenvalue λ_i that we study is simple, which is always the case for $i = 1$. The associated eigenvector u_i is then uniquely defined upon fixing its sign by the condition $(u_i, \chi_i) > 0$, where $\chi_i \in L^2(\Omega)$ is typically a characteristic function of Ω (for $i = 1$) or of its subdomain (for $i > 1$). The setting for $i = 1$ in particular implies the Poincaré–Friedrichs inequality

$$\|v\|^2 \leq \frac{1}{\lambda_1} \|\nabla v\|^2 \qquad \forall v \in V. \tag{2.2}$$

2.2 Meshes and generic piecewise polynomial spaces

We denote by $\mathcal{T}_h$ a matching simplicial mesh in the sense of Ciarlet [24], shape-regular with a parameter $\kappa_{\mathcal{T}} > 0$: the ratio of the element diameter h_K and of the diameter of the inscribed ball to $K \in \mathcal{T}_h$ is bounded by $\kappa_{\mathcal{T}}$ (uniformly for a sequence of meshes). Denote also by h the maximal element diameter over all $K \in \mathcal{T}_h$. The mesh $(d-1)$-dimensional faces are collected in the set $\mathcal{E}_h$, with interior faces $\mathcal{E}_h^{\mathrm{int}}$ and boundary faces $\mathcal{E}_h^{\mathrm{ext}}$. A generic face is denoted by e, its diameter by h_e, and its unit normal vector (the direction is arbitrary but fixed) by $\mathbf{n}_e$. We will often employ the jump operator $[\![\cdot]\!]$ yielding the difference of the traces of the argument from the two mesh elements that share $e \in \mathcal{E}_h^{\mathrm{int}}$ along $\mathbf{n}_e$ and the actual trace for $e \in \mathcal{E}_h^{\mathrm{ext}}$. Similarly, the average operator $\{\!\{\cdot\}\!\}$ yields the mean value of the traces from adjacent mesh elements on interior faces and the actual trace on boundary faces. The set of vertices will be denoted by $\mathcal{V}_h$; it is composed of interior vertices $\mathcal{V}_h^{\mathrm{int}}$ and vertices located on the boundary $\mathcal{V}_h^{\mathrm{ext}}$, with a generic vertex denoted by $\mathbf{a}$.

Let $\mathbb{P}_q(K)$ stand for polynomials of total degree at most $q \geq 0$ on $K \in \mathcal{T}_h$, and $\mathbb{P}_q(\mathcal{T}_h) \subset H^1(\mathcal{T}_h)$ for piecewise q-th order polynomials on $\mathcal{T}_h$. For a given $q \geq 1$, we denote by $V_h^q := \mathbb{P}_q(\mathcal{T}_h) \cap V$ the q-th order conforming finite element space. Similarly, for $q \geq 0$, $\mathbf{V}_h^q := \{\mathbf{v}_h \in \mathbf{H}(\mathrm{div}, \Omega); \mathbf{v}_h|_K \in [\mathbb{P}_q(K)]^d + \mathbb{P}_q(K)\mathbf{x}\}$ and $Q_h^q := \mathbb{P}_q(\mathcal{T}_h)$ stand for the Raviart–Thomas–Nédélec mixed finite element spaces of order q, cf. Brezzi and Fortin [15] or Roberts and Thomas [59]. We will also use the *lowest-order broken space* $\mathbf{V}^0(\mathcal{T}_h) := \{\mathbf{v}_h \in [L^2(\Omega)]^d; \mathbf{v}_h|_K \in [\mathbb{P}_0(K)]^d + \mathbb{P}_0(K)\mathbf{x}\}$, where in contrast to $\mathbf{V}_h^q$, no normal trace continuity is imposed via the inclusion in $\mathbf{H}(\mathrm{div}, \Omega)$.

2.3 Broken and discrete gradients

On the broken Sobolev space $H^1(\mathcal{T}_h)$ defined in (1.2), the usual weak gradient ∇ is not defined. We will in this paper use two successive generalizations of the notion of the weak gradient. We will first denote by

$\nabla_h v \in [L^2(\Omega)]^d$ the *broken gradient* of $v \in H^1(\mathcal{T}_h)$ given by

$$(\nabla_h v)|_K := \nabla(v|_K) \qquad \forall K \in \mathcal{T}_h. \tag{2.3}$$

We will need the following generalization of (2.2), the so-called broken Poincaré–Friedrichs inequality, see Brenner [14, Remark 1.1] or Vohralík [61, Theorem 5.4] and the references therein:

$$\|v\| \le C_{\mathrm{bF}} \left(\|\nabla_h v\|^2 + \sum_{e \in \mathcal{E}_h^{\mathrm{int}}} h_e^{-1} \|\Pi_e^0 [\![v]\!]\|_e^2 + \langle v, 1 \rangle_{\partial\Omega}^2 \right)^{\frac{1}{2}} \qquad \forall v \in H^1(\mathcal{T}_h), \tag{2.4}$$

where Π_e^0 stands for the $L^2(e)$-orthogonal projection onto constants on the face e, $\langle \cdot, \cdot \rangle$ denotes the $L^2(\Omega)$ scalar product over $\partial\Omega$, and the constant C_{bF} only depends on the domain Ω, the space dimension d, and the mesh shape regularity parameter $\kappa_{\mathcal{T}}$.

In order to prove the elliptic regularity bound of Proposition 5.4 below in a very general setting, we are lead to a further generalization. It is motivated by the lifting operators used in the discontinuous Galerkin finite element method, see Di Pietro and Ern [31, Section 4.3] and the references therein, but we crucially rely here on the space $\mathbf{V}^0(\mathcal{T}_h)$ of the lowest-order broken Raviart–Thomas–Nédélec polynomials defined above. Let $v \in H^1(\mathcal{T}_h)$. For each face $e \in \mathcal{E}_h$, we define the lifting operator $\mathfrak{l}_e : L^2(e) \to \mathbf{V}^0(\mathcal{T}_e)$, where $\mathcal{T}_e$ regroups the mesh elements sharing the face e and $\mathbf{V}^0(\mathcal{T}_e)$ is the restriction of $\mathbf{V}^0(\mathcal{T}_h)$ thereon. The lifting $\mathfrak{l}_e([\![v]\!])$ is prescribed by $(\mathfrak{l}_e([\![v]\!]), \mathbf{v}_h)_{\mathcal{T}_e} = \langle \{\!\{\mathbf{v}_h\}\!\} \cdot \mathbf{n}_e, [\![v]\!] \rangle_e$ for all $\mathbf{v}_h \in \mathbf{V}^0(\mathcal{T}_e)$. We then extend $\mathfrak{l}_e([\![v]\!])$ by zero outside of $\mathcal{T}_e$ to form an element of $\mathbf{V}^0(\mathcal{T}_h)$. For a parameter $\theta \in \{-1, 0, 1\}$, the *discrete gradient* $\nabla_\theta v \in [L^2(\Omega)]^d$ is then given by

$$\nabla_\theta v := \nabla_h v - \theta \sum_{e \in \mathcal{E}_h} \mathfrak{l}_e([\![v]\!]). \tag{2.5}$$

We observe that $\nabla_\theta v = \nabla_h v$ when $\theta = 0$ or when the jumps of v are of mean value 0, i.e., $\langle [\![v]\!], 1 \rangle_e = 0$ for all $e \in \mathcal{E}_h$; indeed, this follows from the fact that $\mathbf{v}_h \cdot \mathbf{n}_e$ are constants for $\mathbf{v}_h \in \mathbf{V}^0(\mathcal{T}_h)$. Both broken and discrete gradients are consistent extensions of the weak gradient in the sense that

$$\nabla_\theta v = \nabla_h v = \nabla v \qquad \forall v \in H_0^1(\Omega). \tag{2.6}$$

2.4 Residual and its dual norm

The derivation of a posteriori error estimates usually exploits the concept of the *residual* and of its *dual norm*. We will proceed in this way as well. Throughout the paper, it will turn out to be convenient to employ the residual of different pairs $(w_i, \lambda_{ih}) \in H^1(\mathcal{T}_h) \times \mathbb{R}$, where we take for w_i the approximate solution u_{ih}, the eigenvector reconstruction s_{ih} of Definition 3.3 below, or a generic function in V. Let V' stand for the dual of V.

Definition 2.1 (Residual and its dual norm)**.** *For any pair $(w_i, \lambda_{ih}) \in H^1(\mathcal{T}_h) \times \mathbb{R}$, define the residual $\mathrm{Res}_\theta(w_i, \lambda_{ih}) \in V'$ by*

$$\langle \mathrm{Res}_\theta(w_i, \lambda_{ih}), v \rangle_{V',V} := \lambda_{ih}(w_i, v) - (\nabla_\theta w_i, \nabla v) \qquad \forall v \in V. \tag{2.7a}$$

Its dual norm is then

$$\|\mathrm{Res}_\theta(w_i, \lambda_{ih})\|_{-1} := \sup_{v \in V,\, \|\nabla v\| = 1} \langle \mathrm{Res}_\theta(w_i, \lambda_{ih}), v \rangle_{V',V}. \tag{2.7b}$$

We will also often work with the *Riesz representation* of the residual $\mathfrak{r}_{w_i} \in V$, given by

$$(\nabla \mathfrak{r}_{w_i}, \nabla v) = \langle \mathrm{Res}_\theta(w_i, \lambda_{ih}), v \rangle_{V',V} \qquad \forall v \in V. \tag{2.8a}$$

Then

$$\|\nabla \mathfrak{r}_{w_i}\| = \|\mathrm{Res}_\theta(w_i, \lambda_{ih})\|_{-1}. \tag{2.8b}$$

3 Eigenvector and equilibrated flux reconstructions

We introduce in this section two key reconstructions, following [58, 50, 29, 1, 48, 49, 62, 35, 2, 13, 37, 38] and the references therein. To motivate, note that from (2.1), it is straightforward that $-\nabla u_i \in \mathbf{H}(\mathrm{div},\Omega)$, with the weak divergence equal to $\lambda_i u_i$. On the discrete level, however, $-\nabla_\theta u_{ih} \notin \mathbf{H}(\mathrm{div},\Omega)$ in general, and, a fortiori, $\nabla\cdot(-\nabla_\theta u_{ih}) \neq \lambda_{ih} u_{ih}$. We will thus introduce an *equilibrated flux reconstruction*, a vector-valued function $\boldsymbol{\sigma}_{ih}$ constructed from the given pair (u_{ih},λ_{ih}), satisfying

$$\boldsymbol{\sigma}_{ih} \in \mathbf{H}(\mathrm{div},\Omega), \tag{3.1a}$$

$$\nabla\cdot\boldsymbol{\sigma}_{ih} = \lambda_{ih} u_{ih}. \tag{3.1b}$$

Similarly, as we treat here cases where $u_{ih} \notin V$, possibly jumping between the mesh elements, we will employ an *eigenvector reconstruction*, a scalar-valued function s_{ih} constructed from u_{ih} and satisfying

$$s_{ih} \in V. \tag{3.2}$$

Actually, both $\boldsymbol{\sigma}_{ih}$ and s_{ih} will be piecewise polynomials defined in standard finite element subspaces of $\mathbf{H}(\mathrm{div},\Omega)$ and V, respectively.

3.1 Orthogonality of the residual

Let $\psi_{\mathbf{a}}$ for $\mathbf{a} \in \mathcal{V}_h$ stand for the piecewise affine function taking value 1 at the vertex $\mathbf{a}$ and zero at the other vertices. Remarkably, these functions form a partition of unity via $\sum_{\mathbf{a}\in\mathcal{V}_h} \psi_{\mathbf{a}} = 1|_\Omega$. Denote by $\mathcal{T}_{\mathbf{a}}$ the patch of elements of $\mathcal{T}_h$ which share the vertex $\mathbf{a} \in \mathcal{V}_h$ and by $\omega_{\mathbf{a}}$ the corresponding subdomain of Ω. Recall that $\theta \in \{-1,0,1\}$ is the fixed parameter from the definition of the discrete gradient (2.5). Our key assumption will be:

Assumption 3.1 (Orthogonality of the residual to hat functions)**.** *There holds*

$$\lambda_{ih}(u_{ih},\psi_{\mathbf{a}})_{\omega_{\mathbf{a}}} - (\nabla_\theta u_{ih},\nabla\psi_{\mathbf{a}})_{\omega_{\mathbf{a}}} = \langle \mathrm{Res}_\theta(u_{ih},\lambda_{ih}),\psi_{\mathbf{a}}\rangle_{V',V} = 0 \qquad \forall \mathbf{a} \in \mathcal{V}_h^{\mathrm{int}}.$$

Assumption 3.1 can typically be verified for an exact algebraic solver; Section 7 below shows how to check it for some standard numerical methods. Inexact solvers, where Assumption 3.1 does not hold, can be treated as in [17] and the references therein.

3.2 Reconstruction spaces

In practice, the approximate eigenvector u_{ih} is a piecewise polynomial, $u_{ih} \in \mathbb{P}_p(\mathcal{T}_h)$ for some $p \geq 1$. To define the reconstructions in this setting, we will, for each vertex $\mathbf{a} \in \mathcal{V}_h$, work with restrictions $\mathbf{V}_h^{p+1}(\omega_{\mathbf{a}})$ and $Q_h^{p+1}(\omega_{\mathbf{a}})$ of the spaces from Section 2.2 to the patch subdomain $\omega_{\mathbf{a}}$; conversely, we will often tacitly extend functions defined on $\omega_{\mathbf{a}}$ by zero outside of $\omega_{\mathbf{a}}$. With $\mathbf{n}_{\omega_{\mathbf{a}}}$ standing for the outward unit normal of $\omega_{\mathbf{a}}$, we define

$$\begin{aligned}
&\mathbf{V}_h^{\mathbf{a}} := \{\mathbf{v}_h \in \mathbf{V}_h^{p+1}(\omega_{\mathbf{a}});\ \mathbf{v}_h\cdot\mathbf{n}_{\omega_{\mathbf{a}}} = 0 \text{ on } \partial\omega_{\mathbf{a}}\}, \\
&Q_h^{\mathbf{a}} := \{q_h \in Q_h^{p+1}(\omega_{\mathbf{a}});\ (q_h,1)_{\omega_{\mathbf{a}}} = 0\}, && \mathbf{a} \in \mathcal{V}_h^{\mathrm{int}}, \\
&\mathbf{V}_h^{\mathbf{a}} := \{\mathbf{v}_h \in \mathbf{V}_h^{p+1}(\omega_{\mathbf{a}});\ \mathbf{v}_h\cdot\mathbf{n}_{\omega_{\mathbf{a}}} = 0 \text{ on } \partial\omega_{\mathbf{a}} \setminus \partial\Omega\}, \\
&Q_h^{\mathbf{a}} := Q_h^{p+1}(\omega_{\mathbf{a}}), && \mathbf{a} \in \mathcal{V}_h^{\mathrm{ext}}, \\
&W_h^{\mathbf{a}} := \mathbb{P}_{p+1}(\mathcal{T}_{\mathbf{a}}) \cap H_0^1(\omega_{\mathbf{a}}) && \mathbf{a} \in \mathcal{V}_h.
\end{aligned}$$

3.3 Equilibrated flux reconstruction

We construct $\boldsymbol{\sigma}_{ih}$ satisfying (3.1) by *local constrained minimizations*:

Definition 3.2 (Equilibrated flux reconstruction)**.** *Let $(u_{ih},\lambda_{ih}) \in \mathbb{P}_p(\mathcal{T}_h) \times\mathbb{R}$ be arbitrary but satisfying Assumption 3.1. Prescribe $\boldsymbol{\sigma}_{ih}^{\mathbf{a}} \in \mathbf{V}_h^{\mathbf{a}}$ by solving*

$$\boldsymbol{\sigma}_{ih}^{\mathbf{a}} := \arg \min_{\mathbf{v}_h\in\mathbf{V}_h^{\mathbf{a}},\ \nabla\cdot\mathbf{v}_h = \Pi_{Q_h^{\mathbf{a}}}(\psi_{\mathbf{a}}\lambda_{ih}u_{ih} - \nabla_\theta u_{ih}\cdot\nabla\psi_{\mathbf{a}})} \|\psi_{\mathbf{a}}\nabla_\theta u_{ih} + \mathbf{v}_h\|_{\omega_{\mathbf{a}}} \qquad \forall \mathbf{a} \in \mathcal{V}_h \tag{3.3a}$$

and define

$$\boldsymbol{\sigma}_{ih} := \sum_{\mathbf{a}\in\mathcal{V}_h} \boldsymbol{\sigma}_{ih}^{\mathbf{a}}. \tag{3.3b}$$

In (3.3a), $\Pi_{Q_h^{\mathbf{a}}}$ stands for the $L^2(\Omega)$-orthogonal projection onto the local space $Q_h^{\mathbf{a}}$. It is actually only needed for the simplification of Remark 6.13 below; otherwise, $\psi_{\mathbf{a}}\lambda_{ih}u_{ih} - \nabla_\theta u_{ih}\cdot\nabla\psi_{\mathbf{a}}$ is a piecewise polynomial of degree $p+1$ on the patch $\mathcal{T}_{\mathbf{a}}$, with mean value zero thanks to Assumption 3.1, so that $\Pi_{Q_h^{\mathbf{a}}}(\psi_{\mathbf{a}}\lambda_{ih}u_{ih} - \nabla_\theta u_{ih}\cdot\nabla\psi_{\mathbf{a}}) = \psi_{\mathbf{a}}\lambda_{ih}u_{ih} - \nabla_\theta u_{ih}\cdot\nabla\psi_{\mathbf{a}}$. Imposing the divergence of $\boldsymbol{\sigma}_{ih}^{\mathbf{a}}$ in this way and defining $\boldsymbol{\sigma}_{ih}$ via (3.3b) leads to (3.1b), see, e.g., [38, Lemma 3.5].

It is easy to verify that problems (3.3a) are equivalent (see [38, Remark 3.7]) to the mixed finite element approximation to the homogeneous Neumann (Neumann–Dirichlet close to the boundary) problem posed on the patch $\mathcal{T}_{\mathbf{a}}$: find $\boldsymbol{\sigma}_{ih}^{\mathbf{a}} \in \mathbf{V}_h^{\mathbf{a}}$ and $p_h^{\mathbf{a}} \in Q_h^{\mathbf{a}}$ such that

$$\begin{aligned}
(\boldsymbol{\sigma}_{ih}^{\mathbf{a}}, \mathbf{v}_h)_{\omega_{\mathbf{a}}} - (p_h^{\mathbf{a}}, \nabla\cdot\mathbf{v}_h)_{\omega_{\mathbf{a}}} &= -(\psi_{\mathbf{a}}\nabla_\theta u_{ih}, \mathbf{v}_h)_{\omega_{\mathbf{a}}} && \forall \mathbf{v}_h \in \mathbf{V}_h^{\mathbf{a}},\\
(\nabla\cdot\boldsymbol{\sigma}_{ih}^{\mathbf{a}}, q_h)_{\omega_{\mathbf{a}}} &= (\psi_{\mathbf{a}}\lambda_{ih}u_{ih} - \nabla_\theta u_{ih}\cdot\nabla\psi_{\mathbf{a}}, q_h)_{\omega_{\mathbf{a}}} && \forall q_h \in Q_h^{\mathbf{a}}.
\end{aligned}$$

It follows from the standard references [15, 59] that with the considered choice of the spaces $\mathbf{V}_h^{\mathbf{a}}, Q_h^{\mathbf{a}}$, the discrete inf–sup condition is satisfied.

3.4 Eigenvector reconstruction

For nonconforming eigenvectors u_{ih}, i.e., u_{ih} is a piecewise polynomial not included in $V = H_0^1(\Omega)$ but merely in $H^1(\mathcal{T}_h)$, the eigenvector reconstruction complying with requirement (3.2) is obtained via *local unconstrained minimizations* employing the broken gradient (2.3):

Definition 3.3 (Eigenvector reconstruction)**.** *Let $u_{ih} \in \mathbb{P}_p(\mathcal{T}_h)$ be arbitrary. Prescribe $s_{ih}^{\mathbf{a}} \in W_h^{\mathbf{a}}$ by solving*

$$s_{ih}^{\mathbf{a}} := \arg\min_{v_h\in W_h^{\mathbf{a}}} \|\nabla_h(\psi_{\mathbf{a}}u_{ih} - v_h)\|_{\omega_{\mathbf{a}}} \qquad \forall \mathbf{a}\in\mathcal{V}_h \tag{3.4}$$

and define

$$s_{ih} := \sum_{\mathbf{a}\in\mathcal{V}_h} s_{ih}^{\mathbf{a}}.$$

Problems (3.4) are equivalently described by their Euler–Lagrange conditions; these request to find the conforming finite element approximation $s_{ih}^{\mathbf{a}} \in W_h^{\mathbf{a}}$ to the homogeneous Dirichlet problem posed over the patch $\mathcal{T}_{\mathbf{a}}$ such that

$$(\nabla s_{ih}^{\mathbf{a}}, \nabla v_h)_{\omega_{\mathbf{a}}} = (\nabla_h(\psi_{\mathbf{a}}u_{ih}), \nabla v_h)_{\omega_{\mathbf{a}}} \qquad \forall v_h \in W_h^{\mathbf{a}}.$$

4 Dual norm of the residual and nonconformity bounds

We summarize here bounds on the dual norm of the residual and on nonconformity that are available from the context of source problems. They will be crucial later in Section 6.

4.1 Some additional notation and useful inequalities

We first need to introduce some more background. Consider a vertex $\mathbf{a}\in\mathcal{V}_h$ and on the patch domain $\omega_{\mathbf{a}}$ define

$$H_*^1(\omega_{\mathbf{a}}) := \{v \in H^1(\omega_{\mathbf{a}});\ (v,1)_{\omega_{\mathbf{a}}} = 0\}, \qquad \mathbf{a}\in\mathcal{V}_h^{\mathrm{int}}, \tag{4.1a}$$

$$H_*^1(\omega_{\mathbf{a}}) := \{v \in H^1(\omega_{\mathbf{a}});\ v = 0 \text{ on } \partial\omega_{\mathbf{a}}\cap\partial\Omega\}, \quad \mathbf{a}\in\mathcal{V}_h^{\mathrm{ext}}. \tag{4.1b}$$

Then the *Poincaré–Friedrichs* inequality, corresponding to (2.2) on the patches $\omega_{\mathbf{a}}$, states

$$\|v\|_{\omega_{\mathbf{a}}} \le C_{\mathrm{PF},\omega_{\mathbf{a}}} h_{\omega_{\mathbf{a}}} \|\nabla v\|_{\omega_{\mathbf{a}}} \qquad \forall v \in H_*^1(\omega_{\mathbf{a}}), \tag{4.2a}$$

where $C_{\mathrm{PF},\omega_{\mathbf{a}}}$ depends only on the mesh regularity parameter $\kappa_{\mathcal{T}}$ and the space dimension d. Similarly, when the functions are piecewise H^1 only, we will use the inequality

$$\|v\|_{\omega_{\mathbf{a}}} \le C_{\mathrm{bPF},\omega_{\mathbf{a}}} h_{\omega_{\mathbf{a}}} \left(\|\nabla_h v\|^2_{\omega_{\mathbf{a}}} + \sum_{e\in\mathcal{E}_h,\, \mathbf{a}\in e} h_e^{-1} \|\Pi^0_e [\![v]\!]\|^2_e \right)^{\frac{1}{2}} \tag{4.2b}$$

valid for all $v \in H^1(\mathcal{T}_h)$ such that $(v,1)_{\omega_{\mathbf{a}}} = 0$ when $\mathbf{a} \in \mathcal{V}_h^{\mathrm{int}}$, and where the constant $C_{\mathrm{bPF},\omega_{\mathbf{a}}}$ depends only on $\kappa_{\mathcal{T}}$ and d. Inequality (4.2b) may be seen as a local version of (2.4) on the patch domain $\omega_{\mathbf{a}}$, with the mean value condition $(v,1)_{\omega_{\mathbf{a}}} = 0$ for $\mathbf{a} \in \mathcal{V}_h^{\mathrm{int}}$ or appearance of boundary faces $e \in \mathcal{E}_h \subset \partial\omega_{\mathbf{a}}$ for $\mathbf{a} \in \mathcal{V}_h^{\mathrm{ext}}$. This replaces the boundary term $\langle v, 1\rangle_{\partial\Omega}$ from (2.4). Define $C_{\mathrm{cont,PF}} := \max_{\mathbf{a}\in\mathcal{V}_h}\{1 + C_{\mathrm{PF},\omega_{\mathbf{a}}} h_{\omega_{\mathbf{a}}} \|\nabla\psi_{\mathbf{a}}\|_{\infty,\omega_{\mathbf{a}}}\}$ and $C_{\mathrm{cont,bPF}} := \max_{\mathbf{a}\in\mathcal{V}_h}\{1 + C_{\mathrm{bPF},\omega_{\mathbf{a}}} h_{\omega_{\mathbf{a}}} \|\nabla\psi_{\mathbf{a}}\|_{\infty,\omega_{\mathbf{a}}}\}$. The constants $C_{\mathrm{cont,PF}}$ and $C_{\mathrm{cont,bPF}}$ only depend on the mesh regularity parameter $\kappa_{\mathcal{T}}$ and the space dimension d and can be fully estimated from above, see the discussion in [38, proofs of Lemmas 3.12 and 3.13 and Section 4.3.2]. In particular, there holds, see Carstensen and Funken [19, Theorem 3.1] or Braess *et al.* [12, Section 3]

$$\|\nabla(\psi_{\mathbf{a}} v)\|_{\omega_{\mathbf{a}}} \le C_{\mathrm{cont,PF}} \|\nabla v\|_{\omega_{\mathbf{a}}} \qquad \forall v \in H^1_*(\omega_{\mathbf{a}}),\ \forall \mathbf{a} \in \mathcal{V}_h. \tag{4.3}$$

4.2 Stability of the equilibrated flux and eigenvector reconstructions

Recently, Costabel and McIntosh [25, Corollary 3.4], Demkowicz *et al.* [28, Theorem 7.1], and Demkowicz *et al.* [27, Theorem 6.1] have shown fundamental results on the right inverse of respectively the divergence, the normal trace, and the trace operators for polynomial data on a single (reference) tetrahedron. Therefrom, the two following key *stability* results for the constructions of Definitions 3.2 and 3.3 follow:

$$\|\psi_{\mathbf{a}} \nabla_\theta u_{ih} + \boldsymbol{\sigma}^{\mathbf{a}}_{ih}\|_{\omega_{\mathbf{a}}} \le C_{\mathrm{st}} \sup_{v\in H^1_*(\omega_{\mathbf{a}});\, \|\nabla v\|_{\omega_{\mathbf{a}}}=1} \langle \mathrm{Res}_\theta(u_{ih},\lambda_{ih}), \psi_{\mathbf{a}} v\rangle_{V',V}, \tag{4.4a}$$

$$\|\nabla_h(\psi_{\mathbf{a}} u_{ih} - s^{\mathbf{a}}_{ih})\|_{\omega_{\mathbf{a}}} \le C_{\mathrm{st}} \inf_{v\in H^1_0(\omega_{\mathbf{a}})} \|\nabla_h(\psi_{\mathbf{a}} u_{ih} - v)\|_{\omega_{\mathbf{a}}}, \tag{4.4b}$$

where the constant $C_{\mathrm{st}} > 0$ only depends on the mesh shape regularity parameter $\kappa_{\mathcal{T}}$ and the space dimension d. Indeed, (4.4a) has been shown in Braess *et al.* [12, Theorem 7] in two space dimensions and Ern and Vohralík [39, Corollaries 3.3 and 3.6] in three space dimensions, whereas (4.4b) is proven in [38, Corollary 3.16] in two space dimensions and [39, Corollary 3.1] in three space dimensions. In [39, Corollaries 3.3 and 3.6], we merely need to set $\boldsymbol{\tau}_p = \psi_{\mathbf{a}} \nabla_\theta u_{ih}$, $r_K = \psi_{\mathbf{a}}(\lambda_{ih} u_{ih} + \nabla\cdot(\nabla_\theta u_{ih}))|_K$ for any simplex K in the patch $\mathcal{T}_{\mathbf{a}}$, and $r_F = \psi_{\mathbf{a}} [\![\nabla_\theta u_{ih}]\!]\cdot\mathbf{n}_F$ for any face F in the patch $\mathcal{T}_{\mathbf{a}}$ to infer (4.4a) for interior vertices. Similarly, to see (4.4b), it is enough to take $\tau_p = \psi_{\mathbf{a}} u_{ih}$ and $r_F = \psi_{\mathbf{a}} [\![u_{ih}]\!]_F$ in the notation of [39, Corollary 3.1]. We also remark that computable upper bounds on C_{st} are discussed in [38, Lemma 3.23].

4.3 Dual norm of the residual and nonconformity bounds

Our a posteriori error estimates and their efficiency below will rely on the two following intermediate results:

Corollary 4.1 (Upper and lower bounds on the dual norm of the residual)**.** *Let $(u_{ih},\lambda_{ih}) \in \mathbb{P}_p(\mathcal{T}_h) \times \mathbb{R}^+$ satisfy Assumption 3.1 and let $\boldsymbol{\sigma}_{ih}, s_{ih}$ be respectively constructed following Definitions 3.2 and 3.3. Then*

$$\|\mathrm{Res}_\theta(s_{ih},\lambda_{ih})\|_{-1} \le \left(\frac{\lambda_{ih}}{\sqrt{\lambda_1}} \|u_{ih} - s_{ih}\| + \|\nabla s_{ih} + \boldsymbol{\sigma}_{ih}\| \right), \tag{4.5a}$$

$$\|\nabla_\theta u_{ih} + \boldsymbol{\sigma}_{ih}\| \le (d+1) C_{\mathrm{st}} C_{\mathrm{cont,PF}} \|\mathrm{Res}_\theta(u_{ih},\lambda_{ih})\|_{-1}. \tag{4.5b}$$

Proof. Let $v \in V$ with $\|\nabla v\| = 1$ be fixed. Using the definition of the residual (2.7a), the consistency of the definition of the discrete gradient (2.6), adding and subtracting $(\boldsymbol{\sigma}_{ih}, \nabla v)$, and employing the Green theorem and the equilibrium property (3.1b),

$$\begin{aligned}
\langle \mathrm{Res}_\theta(s_{ih},\lambda_{ih}), v\rangle_{V',V} &= \lambda_{ih}(s_{ih}, v) - (\nabla s_{ih}, \nabla v) \\
&= (\lambda_{ih} s_{ih} - \nabla\cdot\boldsymbol{\sigma}_{ih}, v) - (\nabla s_{ih} + \boldsymbol{\sigma}_{ih}, \nabla v) \\
&= \lambda_{ih}(s_{ih} - u_{ih}, v) - (\nabla s_{ih} + \boldsymbol{\sigma}_{ih}, \nabla v).
\end{aligned}$$

Thus, the characterization (2.7b) of the dual norm of the residual, the Cauchy–Schwarz inequality, and the Poincaré–Friedrichs inequality (2.2) yield (4.5a).

To show (4.5b), let us first note that

$$\begin{aligned}
&\sup_{v\in H^1_*(\omega_{\mathbf{a}});\,\|\nabla v\|_{\omega_{\mathbf{a}}}=1} \langle \mathrm{Res}_\theta(u_{ih},\lambda_{ih}), \psi_{\mathbf{a}} v\rangle_{V',V} \\
&\le \|\mathrm{Res}_\theta(u_{ih},\lambda_{ih})\|_{-1,\omega_{\mathbf{a}}} \sup_{v\in H^1_*(\omega_{\mathbf{a}});\,\|\nabla v\|_{\omega_{\mathbf{a}}}=1} \|\nabla(\psi_{\mathbf{a}} v)\|_{\omega_{\mathbf{a}}} \\
&\le \|\mathrm{Res}_\theta(u_{ih},\lambda_{ih})\|_{-1,\omega_{\mathbf{a}}} C_{\mathrm{cont,PF}},
\end{aligned} \tag{4.6}$$

where $\|\mathrm{Res}_\theta(u_{ih},\lambda_{ih})\|_{-1,\omega_{\mathbf{a}}} := \sup_{v\in H^1_0(\omega_{\mathbf{a}});\,\|\nabla v\|_{\omega_{\mathbf{a}}}=1}\langle \mathrm{Res}_\theta(u_{ih},\lambda_{ih}), v\rangle_{V',V}$, using that for any $v\in H^1_*(\omega_{\mathbf{a}})$, $\psi_{\mathbf{a}} v\in H^1_0(\omega_{\mathbf{a}})$ and (4.3). Since $(\nabla_\theta u_{ih}+\boldsymbol{\sigma}_{ih})|_K = \sum_{\mathbf{a}\in\mathcal{V}_K}(\psi_{\mathbf{a}}\nabla_\theta u_{ih}+\boldsymbol{\sigma}^{\mathbf{a}}_{ih})|_K$ for any $K\in\mathcal{T}_h$, where $\mathcal{V}_K$ stands for the set of the vertices of the element K, and since any simplex has $d+1$ vertices,

$$\begin{aligned}
\|\nabla_\theta u_{ih}+\boldsymbol{\sigma}_{ih}\|^2 &= \sum_{K\in\mathcal{T}_h}\Big\|\sum_{\mathbf{a}\in\mathcal{V}_K}(\psi_{\mathbf{a}}\nabla_\theta u_{ih}+\boldsymbol{\sigma}^{\mathbf{a}}_{ih})\Big\|^2_K \\
&\le (d+1)\sum_{K\in\mathcal{T}_h}\sum_{\mathbf{a}\in\mathcal{V}_K}\|\psi_{\mathbf{a}}\nabla_\theta u_{ih}+\boldsymbol{\sigma}^{\mathbf{a}}_{ih}\|^2_K \\
&= (d+1)\sum_{\mathbf{a}\in\mathcal{V}_h}\|\psi_{\mathbf{a}}\nabla_\theta u_{ih}+\boldsymbol{\sigma}^{\mathbf{a}}_{ih}\|^2_{\omega_{\mathbf{a}}}.
\end{aligned}$$

Now relying on (4.4a) and (4.6), we infer

$$\|\nabla_\theta u_{ih}+\boldsymbol{\sigma}_{ih}\|^2 \le (d+1)C^2_{\mathrm{st}}C^2_{\mathrm{cont,PF}}\sum_{\mathbf{a}\in\mathcal{V}_h}\|\mathrm{Res}_\theta(u_{ih},\lambda_{ih})\|^2_{-1,\omega_{\mathbf{a}}}.$$

Finally, an estimate for combination of negative norms on recovering subdomains, see, for example, [23, Theorem 3.2] and [9, Theorem 3.5] and the references therein, implies (4.5b). □

Corollary 4.2 (Nonconformity lower bound)**.** *For $(u_{ih},\lambda_{ih})\in\mathbb{P}_p(\mathcal{T}_h)\times\mathbb{R}^+$, let s_{ih} be constructed following Definition 3.3. Then*

$$\begin{aligned}
\|\nabla_h(u_{ih}-s_{ih})\| \le \Bigg(&2(d+1)^2C^2_{\mathrm{st}}C^2_{\mathrm{cont,bPF}}\|\nabla_h(u_i-u_{ih})\|^2 \\
&+2d(d+1)C^2_{\mathrm{st}}C^2_{\mathrm{cont,bPF}}\sum_{e\in\mathcal{E}_h}h_e^{-1}\|\Pi^0_e[\![u_{ih}]\!]\|^2_e\Bigg)^{\frac12}.
\end{aligned} \tag{4.7}$$

Proof. This result can be shown as in [38, Lemma 3.22 and Section 4.3.2], relying on (4.2b) and crucially on (4.4b). □

5 Elliptic regularity bounds on the Riesz representation of the residual

An important ingredient for our estimates is a bound on $\|\mathscr{r}_{s_{ih}}\|$ of the Riesz representation $\mathscr{r}_{s_{ih}}\in V$ of the residual $\mathrm{Res}_\theta(s_{ih},\lambda_{ih})$ given by (2.8a). We now derive a sharp estimate on $\|\mathscr{r}_{s_{ih}}\|$ under an elliptic regularity assumption.

Let $\zeta_{(\mathscr{r}_{s_{ih}})}$ be the weak solution of the Laplace *source problem* $-\Delta\zeta_{(\mathscr{r}_{s_{ih}})}=\mathscr{r}_{s_{ih}}$ in Ω and $\zeta_{(\mathscr{r}_{s_{ih}})}=0$ on $\partial\Omega$, i.e., $\zeta_{(\mathscr{r}_{s_{ih}})}\in V$ is such that

$$(\nabla\zeta_{(\mathscr{r}_{s_{ih}})},\nabla v) = (\mathscr{r}_{s_{ih}}, v) \qquad \forall v\in V. \tag{5.1}$$

We will use an Aubin–Nitsche duality argument, see the references in [17, Section 5.1] for the conforming setting and, e.g., Antonietti *et al.* [3, 4] and the references therein for the nonconforming setting. Recalling the lowest-order $H^1_0(\Omega)$- and $\mathbf{H}(\mathrm{div},\Omega)$-conforming finite element spaces V^1_h and $\mathbf{V}^0_h$ from Section 2.2, and denoting Π_0 the $L^2(\Omega)$-orthogonal projection onto piecewise constants, let:

Assumption 5.1 (Elliptic regularity)**.** *The solution $\zeta_{(\mathscr{r}_{s_{ih}})}$ of problem (5.1) belongs to the space $H^{1+\delta}(\Omega)$, $0 < \delta \leq 1$, so that the approximation and stability estimates*

$$\min_{v_h \in V_h^1} \|\nabla(\zeta_{(\mathscr{r}_{s_{ih}})} - v_h)\| \leq C_{\mathrm{I}} h^{\delta} |\zeta_{(\mathscr{r}_{s_{ih}})}|_{H^{1+\delta}(\Omega)}, \tag{5.2a}$$

$$|\zeta_{(\mathscr{r}_{s_{ih}})}|_{H^{1+\delta}(\Omega)} \leq C_{\mathrm{S}} \|\mathscr{r}_{s_{ih}}\| \tag{5.2b}$$

are satisfied. Let moreover, for a suitable $\mathbf{v}_h \in \mathbf{V}_h^0$ such that $\nabla \cdot \mathbf{v}_h = \Pi_0(\mathscr{r}_{s_{ih}})$, the approximation and stability estimates

$$\|\nabla \zeta_{(\mathscr{r}_{s_{ih}})} + \mathbf{v}_h\| \leq \bar{C}_{\mathrm{I}} h^{\delta} |\zeta_{(\mathscr{r}_{s_{ih}})}|_{H^{1+\delta}(\Omega)}, \tag{5.3a}$$

$$\|\mathbf{v}_h\| \leq \bar{C}_{\mathrm{S}} \|\nabla \zeta_{(\mathscr{r}_{s_{ih}})}\| \tag{5.3b}$$

hold. Let finally the inverse inequality

$$\|\mathbf{v}_h \cdot \mathbf{n}_e\|_e \leq C_{\mathrm{inv}} h_e^{-\frac{1}{2}} \|\mathbf{v}_h\|_K \qquad \forall K \in \mathcal{T}_h, \forall e \in \mathcal{E}_K \tag{5.4}$$

hold for all $\mathbf{v}_h \in \mathbf{V}_h^0$, where $\mathcal{E}_K$ stands for the faces of the simplex K.

Remark 5.2 (Constants C_{I} and C_{S})**.** *Let Ω be a convex polygon in two space dimensions. Then it is classical that $\zeta_{(\mathscr{r}_{s_{ih}})} \in H^2(\Omega)$ and $|\zeta_{(\mathscr{r}_{s_{ih}})}|_{H^2(\Omega)} = \|\Delta \zeta_{(\mathscr{r}_{s_{ih}})}\| = \|\mathscr{r}_{s_{ih}}\|$, so that $\delta = 1$ and $C_{\mathrm{S}} = 1$, see Grisvard [41, Theorem 4.3.1.4]. Then, calculable bounds on C_{I} can be found in Liu and Kikuchi [52] and Carstensen* et al. *[21], see also the references therein. In particular, on unstructured triangular meshes, according to [52, equation (46)],*

$$C_{\mathrm{I}} = 0.493 \max_{K \in \mathcal{T}_h} \frac{1 + |\cos(\theta_K)|}{\sin(\theta_K)} \sqrt{\frac{\nu_+(\alpha_K, \theta_K)}{2}} \frac{\tilde{h}_K}{h_K},$$

where $\tilde{h}_K$ is the medium edge length of $K \in \mathcal{T}_h$, $\alpha_K \tilde{h}_K$ is the minimum edge length of K, θ_K is the angle between them, and $\nu_+(\alpha_K, \theta_K) = 1 + \alpha_K^2 + \sqrt{1 + 2\alpha_K^2 \cos 2\theta_K + \alpha_K^4}$, see notation from Section 2, Figure 1, and equations (28), (36), and (46) in [52]. For a mesh formed by isosceles right-angled triangles, $C_{\mathrm{I}} \leq \frac{0.493}{\sqrt{2}}$ from [52].

Remark 5.3 (Constants $\bar{C}_{\mathrm{I}}$, $\bar{C}_{\mathrm{S}}$, and C_{inv})**.** *As above, the ideal case is $\zeta_{(\mathscr{r}_{s_{ih}})} \in H^2(\Omega)$, which happens in particular when Ω is a convex polygon in two space dimensions. Then $\delta = 1$ and calculable bounds on $\bar{C}_{\mathrm{I}}$ can be found in Mao and Shi [54] and Carstensen* et al. *[21] for the choice $\mathbf{v}_h$ as the Raviart–Thomas–Nédélec interpolate of $-\nabla \zeta_{(\mathscr{r}_{s_{ih}})}$. In particular, following [21],*

$$\bar{C}_{\mathrm{I}} = \max_{K \in \mathcal{T}_h} \max_{\alpha \text{ angle of } K} \sqrt{\frac{1/4 + 2/j_{1,1}^2}{1 - |\cos(\alpha)|}}, \tag{5.5}$$

where $j_{1,1} \approx 3.8317059702$ is the first positive root of the Bessel function J_1. This in particular gives $\bar{C}_{\mathrm{I}} = \sqrt{1/4 + 2/j_{1,1}^2} \approx 0.6215$ for a structured mesh with isosceles right-angled triangles. For this interpolate, (5.3b) holds, without any regularity assumption beyond $-\nabla \zeta_{(\mathscr{r}_{s_{ih}})} \in \mathbf{L}^q(\Omega)$, $q > 2$. Finally, (5.4) holds for any $\mathbf{v}_h \in \mathbf{V}_h^0$ and C_{inv} only depends on the shape regularity of the mesh and on the space dimension d, as $\mathbf{v}_h$ is from the lowest-order space.

Proposition 5.4 (Elliptic regularity bound on $\|\mathscr{r}_{s_{ih}}\|$)**.** *Let $(u_{ih}, \lambda_{ih}) \in H^1(\mathcal{T}_h) \times \mathbb{R}^+$ and let Assumptions 3.1 and 5.1 hold. Then*

$$\begin{aligned} \|\mathscr{r}_{s_{ih}}\| \leq{}& \frac{\lambda_{ih}}{\lambda_1} \|u_{ih} - s_{ih}\| + C_{\mathrm{I}} C_{\mathrm{S}} h^{\delta} \|\mathrm{Res}_{\theta}(u_{ih}, \lambda_{ih})\|_{-1} + \bar{C}_{\mathrm{I}} C_{\mathrm{S}} h^{\delta} \|\nabla_{\theta}(u_{ih} - s_{ih})\| \\ &+ \|\Pi_0(u_{ih} - s_{ih})\| + |\theta - 1| \sqrt{d+1} \frac{C_{\mathrm{inv}} \bar{C}_{\mathrm{S}}}{\sqrt{\lambda_1}} \left\{ \sum_{e \in \mathcal{E}_h} h_e^{-1} \|\Pi_e^0 [\![u_{ih}]\!]\|_e^2 \right\}^{\frac{1}{2}}. \end{aligned} \tag{5.6}$$

Proof. By the definition (5.1) of $\zeta_{(\mathscr{r}_{s_{ih}})}$, the definition (2.8a) of $\mathscr{r}_{s_{ih}}$, the definition (2.7a) of $\mathrm{Res}_\theta(s_{ih},\lambda_{ih})$, and the orthogonality Assumption 3.1,

$$\begin{aligned}\|\mathscr{r}_{s_{ih}}\|^2 &= (\nabla\zeta_{(\mathscr{r}_{s_{ih}})},\nabla\mathscr{r}_{s_{ih}}) = \lambda_{ih}(s_{ih},\zeta_{(\mathscr{r}_{s_{ih}})}) - (\nabla s_{ih},\nabla\zeta_{(\mathscr{r}_{s_{ih}})})\\ &= \lambda_{ih}(s_{ih}-u_{ih},\zeta_{(\mathscr{r}_{s_{ih}})}) + \lambda_{ih}(u_{ih},\zeta_{(\mathscr{r}_{s_{ih}})})\\ &\quad - (\nabla_\theta u_{ih},\nabla\zeta_{(\mathscr{r}_{s_{ih}})}) - (\nabla_\theta(s_{ih}-u_{ih}),\nabla\zeta_{(\mathscr{r}_{s_{ih}})})\\ &= \lambda_{ih}(s_{ih}-u_{ih},\zeta_{(\mathscr{r}_{s_{ih}})}) + \lambda_{ih}(u_{ih},\zeta_{(\mathscr{r}_{s_{ih}})}-\zeta_h)\\ &\quad - (\nabla_\theta u_{ih},\nabla(\zeta_{(\mathscr{r}_{s_{ih}})}-\zeta_h)) - (\nabla_\theta(s_{ih}-u_{ih}),\nabla\zeta_{(\mathscr{r}_{s_{ih}})}),\end{aligned}$$

where $\zeta_h\in V_h^1$ is arbitrary. One more application of (2.7a), (2.8a) then leads to

$$\begin{aligned}&\|\mathscr{r}_{s_{ih}}\|^2\\ &= \lambda_{ih}(s_{ih}-u_{ih},\zeta_{(\mathscr{r}_{s_{ih}})}) + (\nabla\mathscr{r}_{u_{ih}},\nabla(\zeta_{(\mathscr{r}_{s_{ih}})}-\zeta_h)) - (\nabla_\theta(s_{ih}-u_{ih}),\nabla\zeta_{(\mathscr{r}_{s_{ih}})})\\ &\le \lambda_{ih}\|s_{ih}-u_{ih}\|\|\zeta_{(\mathscr{r}_{s_{ih}})}\| + \|\nabla\mathscr{r}_{u_{ih}}\|\|\nabla(\zeta_{(\mathscr{r}_{s_{ih}})}-\zeta_h)\| - (\nabla_\theta(s_{ih}-u_{ih}),\nabla\zeta_{(\mathscr{r}_{s_{ih}})}),\end{aligned}$$

where we have also employed the Cauchy–Schwarz inequality. Now the Poincaré–Friedrichs inequality (2.2) gives $\|\zeta_{(\mathscr{r}_{s_{ih}})}\|\le\|\nabla\zeta_{(\mathscr{r}_{s_{ih}})}\|/\sqrt{\lambda_1}$ and we have from (5.1) that $\|\nabla\zeta_{(\mathscr{r}_{s_{ih}})}\|\le\|\mathscr{r}_{s_{ih}}\|/\sqrt{\lambda_1}$. For the second term above, we need to take the best ζ_h and employ the estimates (5.2) to arrive at

$$\begin{aligned}\|\mathscr{r}_{s_{ih}}\|^2 \le &\left(\frac{\lambda_{ih}}{\lambda_1}\|u_{ih}-s_{ih}\| + C_{\mathrm{I}}C_{\mathrm{S}}h^\delta\|\nabla\mathscr{r}_{u_{ih}}\|\right)\|\mathscr{r}_{s_{ih}}\|\\ &- (\nabla\zeta_{(\mathscr{r}_{s_{ih}})},\nabla_\theta(s_{ih}-u_{ih})).\end{aligned}$$

Let now $\mathbf{v}_h\in\mathbf{V}_h^0$ be such that $\nabla\cdot\mathbf{v}_h=\Pi_0(\mathscr{r}_{s_{ih}})$. Definition (2.5) of the discrete gradient and the fact that $\mathbf{v}_h\in\mathbf{V}_h^0\subset\mathbf{V}^0(\mathcal{T}_h)$ give

$$\begin{aligned}-(\mathbf{v}_h,\nabla_\theta u_{ih}) &= -(\mathbf{v}_h,\nabla_h u_{ih}) + \theta\sum_{e\in\mathcal{E}_h}(\mathbf{v}_h,\mathfrak{l}_e([\![u_{ih}]\!]))\\ &= -(\mathbf{v}_h,\nabla_h u_{ih}) + \theta\sum_{e\in\mathcal{E}_h}\langle\{\!\{\mathbf{v}_h\}\!\}\cdot\mathbf{n}_e,[\![u_{ih}]\!]\rangle_e.\end{aligned}$$

Thus, using that $\mathbf{v}_h\in\mathbf{H}(\mathrm{div},\Omega)$ (so that $\{\!\{\mathbf{v}_h\}\!\}\cdot\mathbf{n}_e=\mathbf{v}_h\cdot\mathbf{n}_e$), $s_{ih}\in V$, and elementwise the Green theorem gives

$$(\mathbf{v}_h,\nabla_\theta(s_{ih}-u_{ih})) = -\sum_{K\in\mathcal{T}_h}(\nabla\cdot\mathbf{v}_h,s_{ih}-u_{ih})_K + (\theta-1)\sum_{e\in\mathcal{E}_h}\langle\mathbf{v}_h\cdot\mathbf{n}_e,[\![u_{ih}]\!]\rangle_e.$$

The last term above actually disappears when the jumps of u_{ih} are of mean value 0, i.e., $\langle[\![u_{ih}]\!],1\rangle_e=0$ for all $e\in\mathcal{E}_h$, or when $\theta=1$. As $\mathbf{v}_h\cdot\mathbf{n}_e\in\mathbb{P}_0(e)$, we can, in general, at least replace $[\![u_{ih}]\!]$ by $\Pi_e^0[\![u_{ih}]\!]$ and estimate this term using the inverse inequality (5.4) and Cauchy–Schwarz one, as each simplex has $d+1$ faces

$$\begin{aligned}\left|\sum_{e\in\mathcal{E}_h}\langle\mathbf{v}_h\cdot\mathbf{n}_e,\Pi_e^0[\![u_{ih}]\!]\rangle_e\right| &\le \sum_{e\in\mathcal{E}_h}\left\{\|\mathbf{v}_h\|_{K\in\mathcal{T}_h;\,e\in\mathcal{E}_K}C_{\mathrm{inv}}h_e^{-\frac12}\|\Pi_e^0[\![u_{ih}]\!]\|_e\right\}\\ &\le\sqrt{d+1}C_{\mathrm{inv}}\|\mathbf{v}_h\|\left\{\sum_{e\in\mathcal{E}_h}h_e^{-1}\|\Pi_e^0[\![u_{ih}]\!]\|_e^2\right\}^{\frac12}.\end{aligned}$$

Thus, for $\mathbf{v}_h$ satisfying (5.3) and under the stability assumption (5.2b), we infer

$$
\begin{aligned}
& -(\nabla\zeta_{(\boldsymbol{\imath}_{s_{ih}})}, \nabla_\theta(s_{ih}-u_{ih})) \\
= & -(\nabla\zeta_{(\boldsymbol{\imath}_{s_{ih}})}+\mathbf{v}_h, \nabla_\theta(s_{ih}-u_{ih})) + (\Pi_0(\boldsymbol{\imath}_{s_{ih}}), u_{ih}-s_{ih}) \\
& + (\theta-1)\sum_{e\in\mathcal{E}_h}\langle \mathbf{v}_h\cdot\mathbf{n}_e, \Pi_e^0[\![u_{ih}]\!]\rangle_e \\
= & -(\nabla\zeta_{(\boldsymbol{\imath}_{s_{ih}})}+\mathbf{v}_h, \nabla_\theta(s_{ih}-u_{ih})) + (\boldsymbol{\imath}_{s_{ih}}, \Pi_0(u_{ih}-s_{ih})) \\
& + (\theta-1)\sum_{e\in\mathcal{E}_h}\langle \mathbf{v}_h\cdot\mathbf{n}_e, \Pi_e^0[\![u_{ih}]\!]\rangle_e \\
\le & \bar{C}_{\mathrm{I}}C_{\mathrm{S}}h^\delta\|\boldsymbol{\imath}_{s_{ih}}\|\|\nabla_\theta(u_{ih}-s_{ih})\| + \|\boldsymbol{\imath}_{s_{ih}}\|\|\Pi_0(u_{ih}-s_{ih})\| \\
& + |\theta-1|\sqrt{d+1}\frac{C_{\mathrm{inv}}\bar{C}_{\mathrm{S}}}{\sqrt{\underline{\lambda}_1}}\|\boldsymbol{\imath}_{s_{ih}}\|\left\{\sum_{e\in\mathcal{E}_h} h_e^{-1}\|\Pi_e^0[\![u_{ih}]\!]\|_e^2\right\}^{\frac{1}{2}}.
\end{aligned}
$$

Combining the above estimates with the characterization (2.8b) of $\|\nabla\boldsymbol{\imath}_{u_{ih}}\|$ finishes the proof. □

6 Guaranteed and computable upper and lower bounds in a unified framework

We combine here the results of Sections 4 and 5 together with the key generic equivalences of [17, Section 3] to derive the actual guaranteed and computable eigenvalue and eigenvector bounds in a unified framework.

6.1 Eigenvalues

We first tackle the question of upper and lower bounds for the i-th eigenvalue λ_i. We refer to [17, Remark 5.4 and 5.5] for the discussion on obtaining the auxiliary eigenvalue bounds $\underline{\lambda}_1$, $\overline{\lambda}_{i-1}$, $\overline{\lambda}_i$, and $\underline{\lambda}_{i+1}$.

Theorem 6.1 (Guaranteed lower bounds for the i-th eigenvalue)**.** *Let the i-th exact eigenvalue λ_i, $i\ge 1$, be simple and suppose the auxiliary bounds $\underline{\lambda}_1\le\lambda_1$, $\lambda_i\le\overline{\lambda}_i$, $\underline{\lambda}_{i+1}\le\lambda_{i+1}$, as well as $\lambda_{i-1}\le\overline{\lambda}_{i-1}$ when $i>1$, for $\underline{\lambda}_1,\overline{\lambda}_i,\underline{\lambda}_{i+1},\overline{\lambda}_{i-1}>0$. Let the approximate eigenvector–eigenvalue pair $(u_{ih},\lambda_{ih})\in\mathbb{P}_p(\mathcal{T}_h)\times\mathbb{R}^+$ satisfy Assumption 3.1, as well as the inclusion*

$$
\overline{\lambda}_{i-1}<\lambda_{ih} \text{ when } i>1, \qquad \lambda_{ih}<\underline{\lambda}_{i+1}. \tag{6.1}
$$

Let the equilibrated flux reconstruction $\boldsymbol{\sigma}_{ih}$ be given by Definition 3.2 and the eigenvector reconstruction s_{ih} by Definition 3.3, with $s_{ih}\ne 0$. Denote the principal estimator

$$
\eta_{i,\mathrm{res}} := \frac{1}{\|s_{ih}\|}\left(\frac{\lambda_{ih}}{\sqrt{\underline{\lambda}_1}}\|u_{ih}-s_{ih}\| + \|\nabla s_{ih}+\boldsymbol{\sigma}_{ih}\|\right) \tag{6.2}
$$

together with the discrete relative gaps

$$
c_{ih} := \max\left\{\left(\frac{\lambda_{ih}}{\overline{\lambda}_{i-1}}-1\right)^{-1}, \left(1-\frac{\lambda_{ih}}{\underline{\lambda}_{i+1}}\right)^{-1}\right\}, \tag{6.3a}
$$

$$
\tilde{c}_{ih} := \max\left\{\overline{\lambda}_{i-1}^{-\frac{1}{2}}\left(\frac{\lambda_{ih}}{\overline{\lambda}_{i-1}}-1\right)^{-1}, \underline{\lambda}_{i+1}^{-\frac{1}{2}}\left(1-\frac{\lambda_{ih}}{\underline{\lambda}_{i+1}}\right)^{-1}\right\} \tag{6.3b}
$$

and the scaled eigenvector reconstruction

$$
\tilde{s}_{ih} := \frac{s_{ih}}{\|s_{ih}\|}.
$$

Then, the i-th eigenvalue lower bound is

$$
\boxed{\|\nabla\tilde{s}_{ih}\|^2-\eta_i^2\le\lambda_i}, \tag{6.4}
$$

where the estimator η_i takes different forms in the following three cases:

Case A (No smallness assumption) *If the sign characterization $(u_i, \tilde{s}_{ih}) \geq 0$ is known to hold, the lower i-th eigenvalue estimate (6.4) is valid with*

$$\eta_i^2 := (1 + (\lambda_{ih} + \overline{\lambda}_i)2\tilde{c}_{ih}^2)\eta_{i,\mathrm{res}}^2. \tag{6.5}$$

If only $(\tilde{s}_{ih}, \chi_i) > 0$ holds for the sign characterization function χ_i of Section 2.1, the factor 2 in (6.5) needs to be replaced by $2(1 - \|\tilde{s}_{ih} - \Pi_i \tilde{s}_{ih}\|)^{-1}$, where $\Pi_i \tilde{s}_{ih}$ stands for the $L^2(\Omega)$-orthogonal projection of $\tilde{s}_{ih}$ on the span of χ_i.

Case B (Improved estimates under a smallness assumption) *Assume the sign characterization $(\tilde{s}_{ih}, \chi_i) > 0$ and define*

$$\overline{\alpha}_{ih} := \sqrt{2}\tilde{c}_{ih}\eta_{i,\mathrm{res}}, \tag{6.6a}$$

where $\overline{\alpha}_{ih}$ is a computable bound on the $L^2(\Omega)$ error $\|u_i - \tilde{s}_{ih}\|$. Let the smallness assumption

$$\overline{\alpha}_{ih} \leq \min\left\{\left(\frac{2\underline{\lambda}_1}{\overline{\lambda}_i}\right)^{\frac{1}{2}}, \|\chi_i\|^{-1}(\tilde{s}_{ih}, \chi_i)\right\} \tag{6.6b}$$

hold, so that in particular $\frac{\overline{\lambda}_i}{\underline{\lambda}_1}\frac{\overline{\alpha}_{ih}^2}{4}$ is bounded by $\frac{1}{2}$ and tends to zero; when $i = 1$, taking $\underline{\lambda}_1 = \overline{\lambda}_i = \lambda_i$ is possible and makes the fraction $\frac{\underline{\lambda}_1}{\overline{\lambda}_i}$ vanish. Then the lower i-th eigenvalue estimate (6.4) holds with

$$\eta_i^2 := c_{ih}^2\left(1 - \frac{\overline{\lambda}_i}{\underline{\lambda}_1}\frac{\overline{\alpha}_{ih}^2}{4}\right)^{-1}\eta_{i,\mathrm{res}}^2. \tag{6.7}$$

Case C (Optimal estimates under elliptic regularity assumption) *Assume the elliptic regularity of Assumption 5.1 together with the sign characterization $(\tilde{s}_{ih}, \chi_i) > 0$. Define the $L^2(\Omega)$ estimators $\overline{\alpha}_{ih}$ of $\|u_i - \tilde{s}_{ih}\|$ by*

$$\begin{aligned}\overline{\alpha}_{ih} := \frac{\sqrt{2}c_{ih}}{\|s_{ih}\|}\Bigg(&\frac{\lambda_{ih}}{\underline{\lambda}_1}\|u_{ih} - s_{ih}\| + C_{\mathrm{I}}C_{\mathrm{S}}h^{\delta}\|\nabla_\theta u_{ih} + \boldsymbol{\sigma}_{ih}\| \\ &+ \bar{C}_{\mathrm{I}}C_{\mathrm{S}}h^{\delta}\|\nabla_\theta(u_{ih} - s_{ih})\| + \|\Pi_0(u_{ih} - s_{ih})\| \\ &+ |\theta - 1|\sqrt{d+1}\frac{C_{\mathrm{inv}}\bar{C}_{\mathrm{S}}}{\sqrt{\underline{\lambda}_1}}\left\{\sum_{e\in\mathcal{E}_h} h_e^{-1}\|\Pi_e^0[\![u_{ih}]\!]\|_e^2\right\}^{\frac{1}{2}}\Bigg).\end{aligned} \tag{6.8a}$$

Then, under the smallness assumption

$$\overline{\alpha}_{ih} \leq \|\chi_i\|^{-1}(\tilde{s}_{ih}, \chi_i), \tag{6.8b}$$

the lower i-th eigenvalue estimate (6.4) holds with η_i given by

$$\eta_i^2 := \eta_{i,\mathrm{res}}^2 + (\lambda_{ih} + \overline{\lambda}_i)\overline{\alpha}_{ih}^2. \tag{6.9}$$

Remark 6.2 (Form of the complete estimator η_i)**.** *In Cases A and B above, we immediately see*

$$\eta_i = m_{ih}\eta_{i,\mathrm{res}}, \quad m_{ih} := \begin{cases} (1 + (\lambda_{ih} + \overline{\lambda}_i)2\tilde{c}_{ih}^2)^{\frac{1}{2}} & \text{in Case } A\ , \\ c_{ih}\left(1 - \frac{\overline{\lambda}_i}{\underline{\lambda}_1}\frac{\overline{\alpha}_{ih}^2}{4}\right)^{-\frac{1}{2}} & \text{in Case } B\ , \end{cases}$$

(up to the possible replacement of the factor 2 in Case A) (m_{ih} is bounded by $c_{ih}\sqrt{2}$ and tends to c_{ih} in Case B). Thus the complete estimator η_i indeed takes the form (1.3b) announced in the introduction, where in particular the key role of $\eta_{i,\mathrm{res}}$ given by (6.2) and the unfavorable multiplication by the discrete relative gaps c_{ih} or $\tilde{c}_{ih}$ of (6.3) are obvious. In Case C, η_i^2 rather takes an additive form, with the key estimator $\eta_{i,\mathrm{res}}^2$. Note that $\eta_{i,\mathrm{res}}$ has a leading term (the second one) that comes with constant $1/\|s_{ih}\|$ that tends to the optimal value of one. The other term in $\eta_{i,\mathrm{res}}$ is typically of higher order since it is in the $L^2(\Omega)$-norm (see also Remark 6.9 below). The estimator $\eta_{i,\mathrm{res}}^2$ is supplemented by the term $(\lambda_{ih} + \overline{\lambda}_i)\overline{\alpha}_{ih}^2$. This last term

contains in $\overline{\alpha}_{ih}$ a multiplication by the discrete relative gap c_{ih}. It is, however, typically of higher order whenever the last contribution in $\overline{\alpha}_{ih}$ of (6.8a) disappears, either when the discrete gradient parameter θ from (2.5) is taken as 1 (e.g., symmetric discontinuous Galerkin finite elements), or when the jumps are of mean value zero (e.g., mixed and nonconforming finite elements). This is in particular linked to the terms $\|u_{ih} - s_{ih}\|$ in the $L^2(\Omega)$ norm, see Remark 6.9 below, and to the presence of the δ-power of the maximal element diameter h. Note in this respect that $C_{\mathrm{I}} C_{\mathrm{S}} h^\delta \|\nabla_\theta u_{ih} + \boldsymbol{\sigma}_{ih}\|$ and $\bar{C}_{\mathrm{I}} C_{\mathrm{S}} h^\delta \|\nabla_\theta (u_{ih} - s_{ih})\|$ are still efficient estimates even if $h = const$ (some mesh elements are not refined), see Theorem 6.5 below. Thus, roughly speaking, shall some mesh elements stay unrefined, Case C looses optimal sharpness (the leading term is not only $\eta_{i,\mathrm{res}}$ with the optimal constant one) and Case C sort of degenerates to Case B.

We now prove the three cases of Theorem 6.1 separately:

Proof of Theorem 6.1, **Case A**. It is immediate from estimate (4.5a) of Corollary 4.1 and from definition (6.2) of the principal estimator $\eta_{i,\mathrm{res}}$ together with the scaling $\tilde{s}_{ih} = s_{ih}/\|s_{ih}\|$ that the dual norm of the residual of $(\tilde{s}_{ih}, \lambda_{ih})$ can be estimated as

$$\|\mathrm{Res}_\theta(\tilde{s}_{ih}, \lambda_{ih})\|_{-1} \le \eta_{i,\mathrm{res}}. \tag{6.10}$$

If $(u_i, \tilde{s}_{ih}) \ge 0$ is known to hold, define $\overline{\alpha}_{ih}$ by (6.6a). From [17, Lemma 3.2] in combination with (2.8b), we then infer the $L^2(\Omega)$ bound

$$\|u_i - \tilde{s}_{ih}\| \le \sqrt{2}\tilde{c}_{ih} \|\mathrm{Res}_\theta(\tilde{s}_{ih}, \lambda_{ih})\|_{-1} \le \overline{\alpha}_{ih}. \tag{6.11}$$

Now the upper bound in [17, Theorem 3.4], in combination with the first bound of [17, Theorem 3.5], gives

$$\|\nabla \tilde{s}_{ih}\|^2 - \lambda_i \le \|\nabla(u_i - \tilde{s}_{ih})\|^2 \le \|\mathrm{Res}_\theta(\tilde{s}_{ih}, \lambda_{ih})\|_{-1}^2 + (\lambda_{ih} + \overline{\lambda}_i)\overline{\alpha}_{ih}^2, \tag{6.12}$$

and one more use of (6.10) proves (6.4) with η_i given by (6.5). If only $(\tilde{s}_{ih}, \chi_i) > 0$ holds, we take

$$\overline{\alpha}_{ih} := \sqrt{2}(1 - \|\tilde{s}_{ih} - \Pi_i \tilde{s}_{ih}\|)^{-\frac{1}{2}} \tilde{c}_{ih} \eta_{i,\mathrm{res}}$$

and proceed as in [17, proof of Theorem 5.1, Case A] to find

$$\|u_i - \tilde{s}_{ih}\| \le \sqrt{2}(1 - \|\tilde{s}_{ih} - \Pi_i \tilde{s}_{ih}\|)^{-\frac{1}{2}} \tilde{c}_{ih} \|\mathrm{Res}_\theta(\tilde{s}_{ih}, \lambda_{ih})\|_{-1} \le \overline{\alpha}_{ih}$$

instead of (6.11), and we conclude as above. □

Proof of Theorem 6.1, **Case B**. The second condition in (6.6b) implies that assumptions of [17, Lemma 3.3] are satisfied for $\tilde{s}_{ih}$. Thus the $L^2(\Omega)$ bound (6.11) is valid for $\overline{\alpha}_{ih}$ given by (6.6a). The first condition in (6.6b) then allows us to use the improved estimate in [17, Theorem 3.5]. In combination with the upper bound in [17, Theorem 3.4], this gives

$$\|\nabla \tilde{s}_{ih}\|^2 - \lambda_i \le \|\nabla(u_i - \tilde{s}_{ih})\|^2 \le c_{ih}^2 \left(1 - \frac{\overline{\lambda}_i}{\underline{\lambda}_1} \frac{\overline{\alpha}_{ih}^2}{4}\right)^{-1} \|\mathrm{Res}_\theta(\tilde{s}_{ih}, \lambda_{ih})\|_{-1}^2, \tag{6.13}$$

and we conclude by (6.10). □

Proof of Theorem 6.1, **Case C**. Proposition 5.4 together with the bound $\|\mathrm{Res}_\theta(u_{ih}, \lambda_{ih})\|_{-1} \le \|\nabla_\theta u_{ih} + \boldsymbol{\sigma}_{ih}\|$ and the scaling $\tilde{s}_{ih} = s_{ih}/\|s_{ih}\|$ imply

$$\|\mathscr{r}_{\tilde{s}_{ih}}\| \le \frac{\overline{\alpha}_{ih}}{\sqrt{2} c_{ih}},$$

where $\overline{\alpha}_{ih}$ is given by (6.8a). Next, condition (6.8b) implies that assumptions of [17, Lemma 3.3] are satisfied for $\tilde{s}_{ih}$ and consequently $(u_i, \tilde{s}_{ih}) \ge 0$. Thus [17, Lemma 3.1] again gives the computable $L^2(\Omega)$ bound

$$\|u_i - \tilde{s}_{ih}\| \le \overline{\alpha}_{ih}.$$

We then conclude as in Case A via (6.12). □

Theorem 6.3 (Guaranteed upper bound for the i-th eigenvalue)**.** *For a given $i \geq 1$, let the approximate eigenvectors $u_{kh} \in \mathbb{P}_p(\mathcal{T}_h)$, $1 \leq k \leq i$, be arbitrary, and let s_{kh}, $1 \leq k \leq i$, be their eigenvector reconstructions by Definition 3.3. Suppose that s_{kh}, $1 \leq k \leq i$, are linearly independent. Then*

$$\boxed{\lambda_i \leq \max_{\boldsymbol{\xi} \in \mathbb{R}^i,\, \|\boldsymbol{\xi}\|=1} \frac{\|\nabla \sum_{k=1}^i \boldsymbol{\xi}_k s_{kh}\|^2}{\|\sum_{k=1}^i \boldsymbol{\xi}_k s_{kh}\|^2}}, \tag{6.14}$$

where $\|\boldsymbol{\xi}\|^2 = \sum_{k=1}^i \boldsymbol{\xi}_k^2$. In particular

$$\lambda_1 \leq \frac{\|\nabla s_{1h}\|^2}{\|s_{1h}\|^2} = \|\nabla \tilde{s}_{1h}\|^2. \tag{6.15}$$

Proof. The statement follows immediately from the min–max principle

$$\lambda_i = \min_{V_i \subset V,\, \dim V_i = i} \max_{v \in V_i} \frac{\|\nabla v\|^2}{\|v\|^2}.$$

□

6.2 Eigenvectors

We now turn to the estimates on the error in the approximation of the i-th exact eigenvector u_i by u_{ih} and their efficiency and robustness with respect to the polynomial degree of u_{ih}.

Theorem 6.4 (Guaranteed bounds for the i-th eigenvector error)**.** *Let the assumptions of Theorem 6.1 be satisfied. Then the energy eigenvector error can be bounded via*

$$\boxed{\|\nabla_\theta(u_i - u_{ih})\| \leq \eta_i + \|\nabla_\theta(u_{ih} - \tilde{s}_{ih})\|}, \tag{6.16}$$

where η_i is defined in the three cases A, B, and C respectively by (6.5), (6.7), and (6.9).

Proof. The triangle inequality gives

$$\|\nabla_\theta(u_i - u_{ih})\| \leq \|\nabla_\theta(u_i - \tilde{s}_{ih})\| + \|\nabla_\theta(u_{ih} - \tilde{s}_{ih})\|.$$

We conclude by the bounds $\|\nabla_\theta(u_i - \tilde{s}_{ih})\| = \|\nabla(u_i - \tilde{s}_{ih})\| \leq \eta_i$ shown in (6.12) and (6.13) in the proof of Theorem 6.1. □

Theorem 6.5 (Efficiency and robustness of the estimates)**.** *Let the assumptions of Theorem 6.1 be satisfied. Then estimate (6.16) is efficient as*

$$\boxed{\begin{aligned}\eta_i + \|\nabla_\theta(u_{ih} - \tilde{s}_{ih})\| \leq C_i \Bigg(&\|\nabla_\theta(u_i - u_{ih})\| + \left\{ \sum_{e \in \mathcal{E}_h} h_e^{-1} \|\Pi_e^0 [\![u_{ih}]\!]\|_e^2 \right\}^{\frac{1}{2}} \\ &+ |1 - \|u_{ih}\|| + \left|\lambda_{ih} - \|\nabla_\theta u_{ih}\|^2\right| \Bigg),\end{aligned}} \tag{6.17}$$

where the generic constants C_i can be determined from the detailed estimates:

- *efficiency of $\|\nabla_\theta(u_{ih} - \tilde{s}_{ih})\|$:*

$$\|\nabla_\theta(u_{ih} - \tilde{s}_{ih})\| \leq \|\nabla_\theta(u_{ih} - s_{ih})\| + |1 - \|s_{ih}\|| \frac{\|\nabla s_{ih}\|}{\|s_{ih}\|}, \tag{6.18a}$$

$$\|\nabla_\theta(u_{ih} - s_{ih})\| \leq \|\nabla_h(u_{ih} - s_{ih})\| + |\theta| \sqrt{d+1} C_{\mathrm{inv}} \left\{ \sum_{e \in \mathcal{E}_h} h_e^{-1} \|\Pi_e^0 [\![u_{ih}]\!]\|_e^2 \right\}^{\frac{1}{2}}, \tag{6.18b}$$

  together with (4.7), inequalities (6.21) and (6.19) below, and

$$\|\nabla_h(u_i - u_{ih})\| \leq \|\nabla_\theta(u_i - u_{ih})\| + |\theta| \sqrt{d+1} C_{\mathrm{inv}} \left\{ \sum_{e \in \mathcal{E}_h} h_e^{-1} \|\Pi_e^0 [\![u_{ih}]\!]\|_e^2 \right\}^{\frac{1}{2}}; \tag{6.18c}$$

- *efficiency of* $\|u_{ih} - s_{ih}\|$ *(first part of* $\eta_{i,\mathrm{res}}$*):*

$$\|u_{ih}-s_{ih}\| \le C_{\mathrm{bF}} \left(\|\nabla_h(u_{ih}-s_{ih})\|^2 + \sum_{e\in\mathcal{E}_h^{\mathrm{int}}} h_e^{-1} \|\Pi_e^0 [\![u_{ih}]\!]\|_e^2 + \langle u_{ih}, 1\rangle_{\partial\Omega}^2 \right)^{\frac{1}{2}}, \tag{6.19a}$$

$$|\langle u_{ih}, 1\rangle_{\partial\Omega}| \le h^{\frac{1}{2}} |\partial\Omega|^{\frac{1}{2}} \left\{ \sum_{e\in\mathcal{E}_h^{\mathrm{ext}}} h_e^{-1} \|\Pi_e^0 [\![u_{ih}]\!]\|_e^2 \right\}^{\frac{1}{2}}, \tag{6.19b}$$

together with (4.7) *and* (6.18c)*;*

- *efficiency of* $\|\nabla s_{ih} + \boldsymbol{\sigma}_{ih}\|$ *(second part of* $\eta_{i,\mathrm{res}}$*):*

$$\|\nabla s_{ih} + \boldsymbol{\sigma}_{ih}\| \le \|\nabla_\theta u_{ih} + \boldsymbol{\sigma}_{ih}\| + \|\nabla_\theta(u_{ih} - s_{ih})\|, \tag{6.20a}$$

$$\|\nabla_\theta u_{ih} + \boldsymbol{\sigma}_{ih}\| \le (d+1) C_{\mathrm{st}} C_{\mathrm{cont,PF}} \left(\frac{\lambda_{ih}}{\sqrt{\lambda_1}} \|u_{ih} - s_{ih}\| + \|\nabla_\theta(u_{ih} - s_{ih})\| + \|\mathrm{Res}_\theta(s_{ih}, \lambda_{ih})\|_{-1} \right), \tag{6.20b}$$

$$\|\mathrm{Res}_\theta(s_{ih}, \lambda_{ih})\|_{-1} \le \frac{\|s_{ih}\|}{\sqrt{\lambda_i}} |\lambda_{ih} - \lambda_i| + \overline{C}_{ih}^{\frac{1}{2}} \|s_{ih}\| \|\nabla(u_i - \tilde{s}_{ih})\|, \tag{6.20c}$$

$$\overline{C}_{ih} := 1 \text{ if } i = 1,$$

$$\overline{C}_{ih} := \max\left\{ \left(\frac{\lambda_{ih}}{\lambda_1} - 1 \right)^2, 1 \right\} \text{ if } i > 1,$$

$$|\lambda_{ih} - \lambda_i| \le \|\nabla_\theta(u_i - u_{ih})\|^2 + 2\|\nabla_\theta(u_i - u_{ih})\| \|\nabla_\theta u_{ih}\| + \left| \lambda_{ih} - \|\nabla_\theta u_{ih}\|^2 \right|, \tag{6.20d}$$

together with $\|\nabla(u_i - \tilde{s}_{ih})\| \le \|\nabla_\theta(u_i - u_{ih})\| + \|\nabla_\theta(u_{ih} - \tilde{s}_{ih})\|$*,* (6.18)*,* (6.19)*, and* (6.21) *below;*

- *inequalities for the scaling terms:*

$$|1 - \|s_{ih}\|| \le |1 - \|u_{ih}\|| + \|u_{ih} - s_{ih}\|, \tag{6.21a}$$

$$\|\nabla s_{ih}\| \le \|\nabla_\theta u_{ih}\| + \|\nabla_\theta(u_{ih} - s_{ih})\|, \tag{6.21b}$$

$$\|u_{ih}\| - \|u_{ih} - s_{ih}\| \le \|s_{ih}\| \le \|u_{ih}\| + \|u_{ih} - s_{ih}\|; \tag{6.21c}$$

- *note that* $\overline{\alpha}_{ih}$ *given by* (6.8a) *only contains terms treated above (possibly with multiplicative factors).*

Proof. We first examine the second term on the right-hand side of (6.16). The definition $\tilde{s}_{ih} := \frac{s_{ih}}{\|s_{ih}\|}$ and the triangle inequality give (6.18a), since

$$\|\nabla(s_{ih} - \tilde{s}_{ih})\| = |1 - \|s_{ih}\|| \frac{\|\nabla s_{ih}\|}{\|s_{ih}\|}.$$

As for the first term therein,

$$
\begin{aligned}
\|\nabla_\theta(u_{ih}-s_{ih})\| &= \left\|\nabla_h(u_{ih}-s_{ih}) - \theta\sum_{e\in\mathcal{E}_h} \mathfrak{l}_e([\![u_{ih}]\!])\right\| \\
&\le \|\nabla_h(u_{ih}-s_{ih})\| + |\theta| \left\{\sum_{K\in\mathcal{T}_h}\left\|\sum_{e\in\mathcal{E}_K}\mathfrak{l}_e([\![u_{ih}]\!])\right\|_K^2\right\}^{\frac12} \\
&\le \|\nabla_h(u_{ih}-s_{ih})\| + |\theta| \left\{\sum_{K\in\mathcal{T}_h}(d+1)\sum_{e\in\mathcal{E}_K}\|\mathfrak{l}_e([\![u_{ih}]\!])\|_K^2\right\}^{\frac12} \\
&= \|\nabla_h(u_{ih}-s_{ih})\| + |\theta| \left\{(d+1)\sum_{e\in\mathcal{E}_h}\|\mathfrak{l}_e([\![u_{ih}]\!])\|_{\mathcal{T}_e}^2\right\}^{\frac12},
\end{aligned}
$$

a direct consequence of the definition of the discrete gradient (2.5), of the triangle and Cauchy–Schwarz inequalities, and of the fact that $\mathfrak{l}_e([\![u_{ih}]\!])$ is only supported on the (1 or 2) elements in $\mathcal{T}_e$ containing the face e. Next, the definition of the face lifting $\mathfrak{l}_e$ from Section 2.3, the fact that $\mathbf{v}_h\cdot\mathbf{n}_e$ are constants for $\mathbf{v}_h\in\mathbf{V}^0(\mathcal{T}_e)$, and the inverse inequality (5.4) give

$$
\begin{aligned}
\|\mathfrak{l}_e([\![u_{ih}]\!])\|_{\mathcal{T}_e} &= \sup_{\mathbf{v}_h\in\mathbf{V}^0(\mathcal{T}_e);\,\|\mathbf{v}_h\|_{\mathcal{T}_e}=1} (\mathfrak{l}_e([\![u_{ih}]\!]),\mathbf{v}_h)_{\mathcal{T}_e} \\
&= \sup_{\mathbf{v}_h\in\mathbf{V}^0(\mathcal{T}_e);\,\|\mathbf{v}_h\|_{\mathcal{T}_e}=1} \langle\{\!\{\mathbf{v}_h\}\!\}\cdot\mathbf{n}_e,\Pi_e^0[\![u_{ih}]\!]\rangle_e \\
&\le C_{\mathrm{inv}} h_e^{-\frac12}\|\Pi_e^0[\![u_{ih}]\!]\|_e.
\end{aligned}
$$

Combining the two above bounds gives (6.18b). Finally, (6.18c) follows by, using again (2.5),

$$
\|\nabla_h(u_i-u_{ih})\| = \left\|\nabla_\theta(u_i-u_{ih}) - \theta\sum_{e\in\mathcal{E}_h}\mathfrak{l}_e([\![u_{ih}]\!])\right\|
$$

and proceeding as above for the liftings. Concerning the second term in (6.18a), the multiplicative factor $\|\nabla s_{ih}\|$ approaches $\|\nabla_\theta u_{ih}\|\approx\sqrt{\lambda_{ih}}$ as manifested in (6.21b), the multiplicative factor $\|s_{ih}\|$ is of order 1 when $\|u_{ih}\|\approx 1$ as shown in (6.21c), and $|1-\|s_{ih}\||$ is bounded in (6.21a) by the consistency term $|1-\|u_{ih}\||$ and the estimator $\|u_{ih}-s_{ih}\|$ efficient via (6.19). Thus the efficiency for the term $\|\nabla_\theta(u_{ih}-\tilde{s}_{ih})\|$ as announced in (6.17) follows.

We now turn to the $L^2(\Omega)$-term $\|u_{ih}-s_{ih}\|$, the first part of the estimator $\eta_{i,\mathrm{res}}$ given by (6.2). Note that $\eta_{i,\mathrm{res}}$ forms the principal part of η_i in all three cases A, B, and C, and that the scaling factor $1/\|s_{ih}\|$ is of order 1, see (6.21c). First, (6.19a) is a consequence of the broken Poincaré–Friedrichs inequality (2.4) with $v=u_{ih}-s_{ih}$ and of the fact that the jumps of s_{ih} are zero. The last term in (6.19a) can then still be bounded by

$$
\langle u_{ih},1\rangle_{\partial\Omega}^2 = \left\{\sum_{e\in\mathcal{E}_h^{\mathrm{ext}}}\langle\Pi_e^0[\![u_{ih}]\!],1\rangle_e\right\}^2 \le h\left\{\sum_{e\in\mathcal{E}_h^{\mathrm{ext}}} h_e^{-\frac12}\|\Pi_e^0[\![u_{ih}]\!]\|_e|e|^{\frac12}\right\}^2,
$$

so that (6.19b) follows by another Cauchy–Schwarz inequality. The efficiency of $\|u_{ih}-s_{ih}\|$ is then completed by (4.7) and (6.18c). Numerically, though, we have observed that $\|u_{ih}-s_{ih}\|$ converges still one order faster than what (6.19) suggests, so that it becomes negligible in practice, see Remark 6.9 below.

We now turn to the second part of the estimator $\eta_{i,\mathrm{res}}$ of (6.2), $\|\nabla s_{ih}+\boldsymbol{\sigma}_{ih}\|$. To begin with, (6.20a) follows by the triangle inequality; the second term therein has been treated in (6.18). For $\|\nabla_\theta u_{ih}+\boldsymbol{\sigma}_{ih}\|$, we have the crucial bound (4.5b). As, however, $u_{ih}\notin H_0^1(\Omega)$, we need to get back from $\|\mathrm{Res}_\theta(u_{ih},\lambda_{ih})\|_{-1}$ to $\|\mathrm{Res}_\theta(s_{ih},\lambda_{ih})\|_{-1}$ to prove the efficiency. For this purpose, let $v\in V$ with $\|\nabla v\|=1$ be fixed. Using the residual definition (2.7a), the Cauchy–Schwarz and Poincaré–Friedrichs (2.2) inequalities, and the dual

norm definition (2.7b),

$$\begin{aligned}
&\langle \mathrm{Res}_\theta(u_{ih}, \lambda_{ih}), v\rangle_{V',V} \\
&= \lambda_{ih}(u_{ih}, v) - (\nabla_\theta u_{ih}, \nabla v) \\
&= \lambda_{ih}(u_{ih} - s_{ih}, v) - (\nabla_\theta(u_{ih} - s_{ih}), \nabla v) + \langle \mathrm{Res}_\theta(s_{ih}, \lambda_{ih}), v\rangle_{V',V} \\
&\le \frac{\lambda_{ih}}{\sqrt{\lambda_1}}\|u_{ih} - s_{ih}\| + \|\nabla_\theta(u_{ih} - s_{ih})\| + \|\mathrm{Res}_\theta(s_{ih}, \lambda_{ih})\|_{-1},
\end{aligned}$$

so that (6.20b) follows. We know from (6.18) and (6.19) that the first two terms herein are efficient, so that we pursue with the last one only. To start with, note that $\|\mathrm{Res}_\theta(s_{ih}, \lambda_{ih})\|_{-1} = \|s_{ih}\|\|\mathrm{Res}_\theta(\tilde{s}_{ih}, \lambda_{ih})\|_{-1}$; then (6.20c) follows from the proof of the second bound in [17, Theorem 3.5]. To finish, develop

$$\begin{aligned}
\lambda_{ih} - \lambda_i &= \lambda_{ih} - \|\nabla_\theta(u_i - u_{ih} + u_{ih})\|^2 \\
&= \lambda_{ih} - \|\nabla_\theta(u_i - u_{ih})\|^2 - 2(\nabla_\theta(u_i - u_{ih}), \nabla_\theta u_{ih}) - \|\nabla_\theta u_{ih}\|^2,
\end{aligned}$$

which proves (6.20d) and together with (6.18), (6.19), and (6.21) gives the requested efficiency. □

6.3 Comments

We now give some comments on the results of Theorems 6.1–6.5; a discussion for the conforming setting can be found in [17, Section 5.3].

Remark 6.6 (Vanishing consistency terms)**.** *Nonconforming finite elements are a particular example of a numerical method where both consistency terms* $|1 - \|u_{ih}\||$ *and* $\left|\lambda_{ih} - \|\nabla_\theta u_{ih}\|^2\right|$ *are zero and thus vanish in* (6.17)*, see Section 7.1 below.*

Remark 6.7 (Jumps of mean value zero)**.** *A particular situation arises when* $\langle [\![u_{ih}]\!], 1\rangle_e = 0$ *for all* $e \in \mathcal{E}_h$*, i.e., when the jumps over the mesh faces in the eigenvector approximation vanish in mean value. Then the discrete and broken gradient coincide, i.e.,* $\nabla_\theta = \nabla_h$ *(see Section 2.3) and all the mean value jump terms of the form* $h_e^{-\frac{1}{2}}\|\Pi_e^0[\![u_{ih}]\!]\|_e$ *of the present paper vanish, in particular in* (6.8a) *and in* (6.17)*. Moreover,* (4.7) *and* (6.19a) *simplify respectively to*

$$\|\nabla_h(u_{ih} - s_{ih})\| \le (d+1)C_{\mathrm{st}}C_{\mathrm{cont,bPF}}\|\nabla_h(u_i - u_{ih})\|, \tag{6.22a}$$

$$\|u_{ih} - s_{ih}\| \le (d+1)C_{\mathrm{st}}C_{\mathrm{cont,bPF}}C_{\mathrm{bF}}\|\nabla_h(u_i - u_{ih})\|, \tag{6.22b}$$

see [38, Lemma 3.22 and Section 4.3.2]. This very favorable context arises namely for nonconforming and mixed finite elements, as we will see below in Sections 7.1 and 7.3.

Remark 6.8 (Jump-free estimators for the symmetric discontinuous Galerkin method)**.** *The jump terms in the estimator* $\overline{\alpha}_{ih}$ *given by* (6.8a) *also vanish when* $\theta = 1$*, which is typically the situation for the symmetric discontinuous Galerkin method of Section 7.2 below.*

Remark 6.9 (Alternative mean-value-preserving eigenvector reconstruction)**.** *The term* $\frac{\lambda_{ih}}{\sqrt{\lambda_1}}\|u_{ih} - s_{ih}\|$ *in* (4.5a)*,* (6.2)*, and* (6.8a) *with the eigenvector reconstruction* s_{ih} *of Definition 3.3 typically converges by one order faster than* $\|\nabla s_{ih} + \boldsymbol{\sigma}_{ih}\|$*, while allowing to prove polynomial degree robustness. One could additionally impose* s_{ih} *to be elementwise of the same mean value as* u_{ih}*, see [36, (3.2) and (3.16)]. Then* $\frac{\lambda_{ih}}{\sqrt{\lambda_1}}\|u_{ih} - s_{ih}\|$ *can be replaced by* $\frac{\lambda_{ih}}{\pi}\left\{\sum_{K\in\mathcal{T}_h}(h_K\|u_{ih} - s_{ih}\|_K)^2\right\}^{\frac{1}{2}}$*, with an additional mesh power. Indeed, in this case* $\lambda_{ih}(s_{ih} - u_{ih}, v) = \lambda_{ih}\sum_{K\in\mathcal{T}_h}(s_{ih} - u_{ih}, v - \Pi_0 v)_K \le \lambda_{ih}\sum_{K\in\mathcal{T}_h}(\|s_{ih} - u_{ih}\|_K\frac{h_K}{\pi}\|\nabla v\|_K)$ *in the proof of Corollary 4.1, by the Poincaré inequality and convexity of simplices.*

Remark 6.10 (Alternative eigenvector reconstruction and vanishing jumps for the symmetric discontinuous Galerkin method)**.** *An alternative eigenvector reconstruction to that of Definition 3.3 is possible in two space dimensions following [38, Remark 3.11] when* $\left(\nabla_\theta u_{ih}, \begin{pmatrix} 0 & -1 \\ 1 & 0 \end{pmatrix}\nabla\psi_{\mathbf{a}}\right)_{\omega_{\mathbf{a}}} = 0$ *for all* $\mathbf{a} \in \mathcal{V}_h$*. This is in particular satisfied for the symmetric variant of the discontinuous Galerkin method of Section 7.2 below. This alternative reconstruction remarkably yields*

$$\|\nabla_\theta(u_{ih} - s_{ih})\| \le (d+1)C_{\mathrm{st}}C_{\mathrm{cont,P}}\|\nabla_\theta(u_i - u_{ih})\|$$

in place of (6.18b), (4.7), *and* (6.18c). *Here the constant* $C_{\mathrm{cont,P}} := \max_{\mathbf{a}\in\mathcal{V}_h}\{1 + C_{\mathrm{P},\omega_\mathbf{a}} h_{\omega_\mathbf{a}} \|\nabla\psi_\mathbf{a}\|_{\infty,\omega_\mathbf{a}}\}$ *with* $C_{\mathrm{P},\omega_\mathbf{a}}$ *given by* (4.2a) *where zero mean value condition* $(v,1)_{\omega_\mathbf{a}} = 0$ *is also imposed for boundary vertices. This is an equivalent of the bound* (6.22a), *again without any jump terms. Then, all the principal estimators are efficient without any jump term, fully mimicking the situation of Remark 6.7.*

Remark 6.11 (Optimal efficiency and polynomial-degree robustness)**.** *Theorem 6.5 shows that both estimators* η_i *and* $\|\nabla_\theta(u_{ih} - \tilde{s}_{ih})\|$ *are equivalent to the eigenvector energy error* $\|\nabla_\theta(u_i - u_{ih})\|$ *for nonconforming finite elements, see Remarks 6.6 and 6.7. A similar case can arise for the symmetric discontinuous Galerkin method, see Remark 6.10. Taking into account that the size of our confidence interval for the* i*-th eigenvalue of Theorem 6.1 is* η_i^2*, this gives a fully optimal theory with in particular* polynomial-degree-robustness*. In the general case, the jumps in mean values of* u_{ih}*,* $\{\sum_{e\in\mathcal{E}_h} h_e^{-1}\|\Pi_e^0[\![u_{ih}]\!]\|_e^2\}^{\frac{1}{2}}$*, may be added to the error in the form* $\{\sum_{e\in\mathcal{E}_h} h_e^{-1}\|\Pi_e^0[\![u_i - u_{ih}]\!]\|_e^2\}^{\frac{1}{2}}$*, as typically done in discontinuous Galerkin methods, and similarly for the consistency terms, so as to still have equivalence between the eigenvector energy error and its estimate.*

Remark 6.12 (Negative influence of the discrete relative gap and decreasing efficiency for increasing eigenvalues)**.** *The efficiency constant* C_i *in* (6.17) *unfortunately contains the discrete relative gap* c_{ih} *or* $\tilde{c}_{ih}$ *of* (6.3)*, since these are included as multiplicative factors in the complete estimator* η_i*, see Remark 6.2. Only in Case C when the discrete gradient parameter* θ *from* (2.5) *is taken as* 1 *(e.g., symmetric discontinuous Galerkin finite elements) or when the jumps are of mean value zero (e.g., mixed and nonconforming finite elements), see Remark 6.2, and when* $\|u_{ih} - s_{ih}\|$ *and consequently* $\|\Pi_0(u_{ih} - s_{ih})\|$ *decay at least as* $h^\delta\|\nabla_\theta u_{ih} + \boldsymbol{\sigma}_{ih}\|$*, the influence of these discrete relative gaps vanishes with the maximal mesh size* h *tending to zero. Moreover, the factor* $\overline{C}_{ih}$ *from* (6.20c) *deteriorates the efficiency for increasing eigenvalues, except in our mixed finite elements setting of Section 7.3 where it does not appear.*

Remark 6.13 (Cheaper flux and potential reconstructions)**.** *The lower bound* (6.4) *for eigenvalues and the upper bound* (6.16) *for eigenvectors stay valid for cheaper (by one polynomial degree) flux and potential reconstructions, where* $\mathbf{V}_h^p(\omega_\mathbf{a}) \times Q_h^p(\omega_\mathbf{a})$ *and* $\mathbb{P}_p(\mathcal{T}_\mathbf{a}) \cap H_0^1(\omega_\mathbf{a})$ *are used in Section 3.2, instead of* $\mathbf{V}_h^{p+1}(\omega_\mathbf{a}) \times Q_h^{p+1}(\omega_\mathbf{a})$ *and* $\mathbb{P}_{p+1}(\mathcal{T}_\mathbf{a}) \cap H_0^1(\omega_\mathbf{a})$*. This is often completely sufficient in practice, albeit the theoretical polynomial degree robustness* (6.17) *may be lost. We employ these cheaper reconstructions in our numerical experiments in Section 8 below.*

7 Application to common nonconforming numerical methods

We verify in this section the conditions of the application of our results to three common nonconforming numerical discretizations of the Laplace eigenvalue problem (2.1).

7.1 Nonconforming finite elements

Let V_h be spanned by functions v_h from $\mathbb{P}_p(\mathcal{T}_h)$, $p \geq 1$, such that $\langle [\![v_h]\!], q_h\rangle_e = 0$ for all $q_h \in \mathbb{P}_{p-1}(e)$ and all $e \in \mathcal{E}_h$. The nonconforming finite element method for problem (2.1) reads, cf. [26, 45, 46, 20, 63]: find $(u_{ih}, \lambda_{ih}) \in V_h \times \mathbb{R}^+$ with $(u_{ih}, u_{jh}) = \delta_{ij}$, $1 \leq i, j \leq \dim V_h$, such that

$$(\nabla_h u_{ih}, \nabla_h v_h) = \lambda_{ih}(u_{ih}, v_h) \qquad \forall v_h \in V_h; \tag{7.1}$$

the sign of the eigenvector u_{ih} is fixed by $(u_{ih}, \chi_i) > 0$. As the jump mean values in the space V_h are zero, $\nabla_\theta = \nabla_h$ follows from (2.5) (we can, e.g., take $\theta = 0$). Then definition (7.1) directly implies Assumption 3.1 (take $v_h = \psi_\mathbf{a} \in V_h$ in (7.1)). Thus, upon the verification/satisfaction of condition (6.6b) (in Case B) and of (6.8b) (in Case C), all the results of Theorems 6.1–6.5 hold. We actually have clear eigenvector efficiency without jumps and consistency terms ($\lambda_{ih} = \|\nabla_h u_{ih}\|^2$ follows by taking $v_h = u_{ih}$ in (7.1)), see Remarks 6.6 and 6.7, and optimally convergent eigenvalue and eigenvector bounds, see Remark 6.11.

7.2 Discontinuous Galerkin finite elements

Set $V_h := \mathbb{P}_p(\mathcal{T}_h)$, $p \geq 1$, without any continuity requirement. The discontinuous Galerkin finite element method for problem (2.1), cf. [3, 40] and the references therein, reads: find $(u_{ih}, \lambda_{ih}) \in V_h \times \mathbb{R}^+$ with

$(u_{ih}, u_{jh}) = \delta_{ij}$, $1 \le i, j \le \dim V_h$, such that

$$\begin{aligned} &\sum_{K\in\mathcal{T}_h} (\nabla_h u_{ih}, \nabla_h v_h)_K - \sum_{e\in\mathcal{E}_h} \{\langle \{\!\{\nabla_h u_{ih}\}\!\}\cdot\mathbf{n}_e, [\![v_h]\!]\rangle_e + \theta\langle \{\!\{\nabla_h v_h\}\!\}\cdot\mathbf{n}_e, [\![u_{ih}]\!]\rangle_e\} \\ &+ \sum_{e\in\mathcal{E}_h} \langle \nu h_e^{-1}[\![u_{ih}]\!], [\![v_h]\!]\rangle_e = \lambda_{ih}(u_{ih}, v_h) \qquad \forall v_h \in V_h; \end{aligned} \tag{7.2}$$

the sign of u_{ih} is fixed by $(u_{ih}, \chi_i) > 0$. Here ν is a positive stabilization parameter and the parameter $\theta \in \{-1, 0, 1\}$ defines the discrete gradient (2.5) in Section 2.3 and corresponds respectively to the nonsymmetric, incomplete, and symmetric variants. The system matrix corresponding to (7.2) is only symmetric for $\theta = 1$. In the other cases, we tacitly assume that the i-th eigenvalue λ_{ih} that one computes is real. This typically happens for the first eigenvalue and more generally for all simple eigenvalues, cf. the numerical experiments in [3, Section 7.1.2].

With the concept of the discrete gradient (2.5), the orthogonality of Assumption 3.1 is immediately satisfied. Indeed, it is enough to take $v_h = \psi_{\mathbf{a}} \in V_h$ in (7.2) and take into account the facts that $\psi_{\mathbf{a}}$ has no jumps as well as that $\nabla\psi_{\mathbf{a}} \in [\mathbb{P}_0(\mathcal{T}_h)]^d \subset \mathbf{V}^0(\mathcal{T}_h)$. Thus all the results of Theorems 6.1–6.5 hold upon the satisfaction of their assumptions. Recall also that 1) for $\theta = 0$, the broken ∇_h and discrete ∇_θ gradients coincide; 2) the jumps are here generally not of mean value zero, $\langle [\![u_{ih}]\!], 1\rangle_e \neq 0$ for $e \in \mathcal{E}_h$, so that Remark 6.7 does not apply here; 3) the choice $\theta = 1$ leads to a remarkable situation where the jumps vanish from $\overline{\alpha_{ih}}$ given by (6.8a) and consequently from all three considered estimators η_i in Theorems 6.1 and 6.4, see Remark 6.8; 4) the choice $\theta = 1$ and the alternative eigenvector reconstruction of Remark 6.10 make the jumps vanish also from all the important parts in the efficiency bounds of Theorem 6.5.

7.3 Mixed finite elements

Let $\overline{\mathbf{V}}_h \times \overline{Q}_h$ be any pair of the usual mixed finite element spaces, see [15, 59] and also Section 2.2 for the Raviart–Thomas–Nédélec case. The mixed finite element method for problem (2.1) looks for the triple $\overline{\boldsymbol{\sigma}}_{ih} \in \overline{\mathbf{V}}_h$, $\bar{u}_{ih} \in \overline{Q}_h$, and $\lambda_{ih} \in \mathbb{R}^+$ such that $(u_{ih}, u_{jh}) = \delta_{ij}$, $1 \le i, j \le \dim \overline{Q}_h$, and, cf. [56, 34, 11, 47] and the references therein,

$$(\overline{\boldsymbol{\sigma}}_{ih}, \mathbf{v}_h) - (\bar{u}_{ih}, \nabla\cdot\mathbf{v}_h) = 0 \qquad \forall \mathbf{v}_h \in \overline{\mathbf{V}}_h, \tag{7.3a}$$

$$(\nabla\cdot\overline{\boldsymbol{\sigma}}_{ih}, q_h) = \lambda_{ih}(\bar{u}_{ih}, q_h) \qquad \forall q_h \in \overline{Q}_h, \tag{7.3b}$$

where the sign of the i-th eigenvector that we are interested in is fixed by $(\bar{u}_{ih}, \chi_i) > 0$.

The low-order eigenvector approximation $\bar{u}_{ih}$ is typically elementwise postprocessed in mixed finite element methods. In particular, following Arnold and Brezzi [7], Arbogast and Chen [5], and Vohralík [62], there exists for each pair $\overline{\mathbf{V}}_h \times \overline{Q}_h$ a piecewise polynomial space M_h such that $u_{ih} \in M_h$ can be prescribed by

$$\Pi_{\overline{Q}_h(K)}(u_{ih}|_K) = \bar{u}_{ih}|_K \qquad \forall K \in \mathcal{T}_h, \tag{7.4a}$$

$$\Pi_{\overline{\mathbf{V}}_h(K)}((-\nabla_h u_{ih})|_K) = \overline{\boldsymbol{\sigma}}_{ih}|_K \qquad \forall K \in \mathcal{T}_h, \tag{7.4b}$$

where $\Pi_{\overline{Q}_h(K)}$ is the $L^2(K)$-orthogonal projection onto $\overline{Q}_h(K)$ and $\Pi_{\overline{\mathbf{V}}_h(K)}$ is the $[L^2(K)]^d$-orthogonal projection onto $\overline{\mathbf{V}}_h(K)$. Let p denote the polynomial degree of the approximation u_{ih} resulting from (7.4), i.e., $u_{ih} \in \mathbb{P}_p(\mathcal{T}_h)$ as throughout the paper. A remarkable fact is that (7.4) and (7.3a) imply

$$\langle [\![u_{ih}]\!], v_h\rangle_e = 0 \qquad \forall v_h \in \overline{\mathbf{V}}_h\cdot\mathbf{n}_e(e),\ \forall e \in \mathcal{E}_h,$$

so that in particular the zero mean-value condition, cf. Remark 6.7, is satisfied. Consequently, $\nabla_\theta = \nabla_h$, see (2.5) (and we can, e.g., take $\theta = 0$). The computed flux $\overline{\boldsymbol{\sigma}}_{ih}$ can typically serve directly as an equilibrated flux reconstruction in mixed finite elements, see [38, Section 4.4] and the references therein. However, in the present eigenvalue case, it only follows from (7.3b) that $\nabla\cdot\overline{\boldsymbol{\sigma}}_{ih} = \lambda_{ih}\bar{u}_{ih}$, and not $\nabla\cdot\overline{\boldsymbol{\sigma}}_{ih} = \lambda_{ih}u_{ih}$ as requested in the equilibrium property (3.1b) and necessary in the proof of the upper bound (4.5a). We can, however, postprocess elementwise the flux $\overline{\boldsymbol{\sigma}}_{ih}$ as well: choose a mixed space $\mathbf{V}_h^q$ with a sufficient polynomial degree q such that $M_h \subset \nabla\cdot\mathbf{V}_h^q$. Denoting by $\mathbf{n}_K$ the outward unit normal to K, define

$$\boldsymbol{\sigma}_{ih}|_K := \arg \min_{\substack{\mathbf{v}_h\in\mathbf{V}_h^q(K),\ \mathbf{v}_h\cdot\mathbf{n}_K=\overline{\boldsymbol{\sigma}}_{ih}\cdot\mathbf{n}_K \text{ on } \partial K \\ \nabla\cdot\mathbf{v}_h=\lambda_{ih}u_{ih}}} \|\overline{\boldsymbol{\sigma}}_{ih} - \mathbf{v}_h\|_K \qquad \forall K \in \mathcal{T}_h \tag{7.5}$$

instead of (3.3a) of Definition 3.2. The well-posedness of (7.5) follows from (7.3b) and (7.4a). Note that $\boldsymbol{\sigma}_{ih}$ is only a slight local elementwise modification of $\overline{\boldsymbol{\sigma}}_{ih}$, preserving the normal component while improving the divergence.

With the just described setting, all the eigenvalue results of Section 6 hold true in the following sense:

Corollary 7.1 (Eigenvalue bounds for mixed finite elements)**.** *Let $\underline{\lambda}_1, \overline{\lambda}_i$, $\underline{\lambda}_{i+1}, \overline{\lambda}_{i-1} > 0$ be the auxiliary bounds as in Theorem 6.1. Let (u_{ih}, λ_{ih}) be given by (7.3)–(7.4). Construct s_{ih} from u_{ih} following Definition 3.3 and $\boldsymbol{\sigma}_{ih}$ by (7.5). Then, the bounds (6.4) and (6.14) of respectively Theorems 6.1 and 6.3 hold true (in the three cases A, B, and C).*

Concerning the eigenvectors, the guaranteed upper bounds (4.5a) and consequently (6.16) do hold even if u_{ih} does not satisfy Assumption 3.1; the key is that $\nabla\cdot\boldsymbol{\sigma}_{ih} = \lambda_{ih} u_{ih}$ that we have arranged in (7.5). For the efficiency, recall first that $\nabla_\theta = \nabla_h$, so that (6.18b) and (6.18c) are redundant here. Next, the bounds (4.7) and (6.19), or more precisely their improvements (6.22), only exploit the construction of s_{ih} from u_{ih} via Definition 3.3 and are thus also valid. Unfortunately, (4.5b) and consequently (6.20) do not hold in general, as $\boldsymbol{\sigma}_{ih}$ is not constructed from u_{ih} by Definition 3.2 but via (7.5). In order to restore fully optimal (guaranteed, efficient, and polynomial-degree robust) eigenvector error control, we proceed as in [38, Section 4.4], see also the references therein. Invoking the triangle inequality $\|\nabla u_i + \boldsymbol{\sigma}_{ih}\| \le \|\nabla_h(u_i - u_{ih})\| + \|\nabla_h u_{ih} + \boldsymbol{\sigma}_{ih}\|$, we have the following optimal simultaneous error control in $\nabla_h u_{ih}$ and $-\boldsymbol{\sigma}_{ih}$:

Corollary 7.2 (Eigenvector bounds for mixed finite elements)**.** *Let the assumptions of Corollary 7.1 be satisfied. Then, in the three cases A, B, and C of Theorem 6.1,*

$$\|\nabla_h(u_i - u_{ih})\| + \|\nabla u_i + \boldsymbol{\sigma}_{ih}\| \le 2(\eta_i + \|\nabla_h(u_{ih} - \tilde{s}_{ih})\|) + \|\nabla_h u_{ih} + \boldsymbol{\sigma}_{ih}\|.$$

This bound is efficient as (6.22) holds together with

$$\|\nabla_h u_{ih} + \boldsymbol{\sigma}_{ih}\| \le \|\nabla_h(u_i - u_{ih})\| + \|\nabla u_i + \boldsymbol{\sigma}_{ih}\|.$$

8 Numerical experiments

We now numerically illustrate our estimates on two test cases in $\mathbb{R}^2$, for the nonconforming finite element method of order $p = 1$ and the symmetric ($\theta = 1$) discontinuous Galerkin finite element method of order $p = 1$ and $p = 2$. We actually only study the first eigenpair; results for the higher eigenpairs are similar as in [17]. For the discontinuous Galerkin method, we consider two different pairs of the auxiliary bounds $\underline{\lambda}_1$ and $\underline{\lambda}_2$, to showcase the sensitivity of our bounds with respect to them. We use the cheaper Raviart–Thomas–Nédélec space of degree p for the flux equilibration instead of $p + 1$, as discussed in Remark 6.13. This still gives guaranteed bounds and we do not observe any asymptotic loss of efficiency. The implementation was done in the FreeFem++ code [42, 43]. If the additional elliptic regularity for the corresponding source problem of Assumption 5.1 holds, so that Case C of Theorems 6.1 and 6.4 can be used, we observe that the last term of (6.8a) vanishes in the two considered numerical methods. We exploit in this case (the unit square below) full $H^2(\Omega)$ regularity and use the constants $C_{\mathrm{S}} = 1$ and $\delta = 1$ given in Remark 5.2 and set C_{I} and $\bar{C}_{\mathrm{I}}$ following respectively Remarks 5.2 and 5.3.

8.1 Nonconforming finite element method

We test here the performance of the lowest-order ($p = 1$) nonconforming finite element method as described in Section 7.1. Recall that the jump mean values are zero here, so that $\nabla_\theta = \nabla_h$ from (2.5); we take $\theta = 0$.

8.1.1 Unit square

We start by testing the framework on a geometry where everything is known explicitly: the unit square $\Omega = (0, 1)^2$. The eigenvalues on a square of size H being $\pi^2(k^2+l^2)/H^2$, $k, l \in \mathbb{N}^\star$, the first and second eigenvalues are $\lambda_1 = 2\pi^2$ and $\lambda_2 = 5\pi^2$, respectively. The first eigenfunction is given by $u_1(x, y) = 2\sin(\pi x)\sin(\pi y)$. We can here apply the refined elliptic regularity of Case C, since $d = 2$ and the domain is convex; we also compare it to the Case B. We set $\underline{\lambda}_1 := 1.5\pi^2 < \lambda_1$, $\underline{\lambda}_2 := 4.5\pi^2 < \lambda_2$, and $\overline{\lambda}_1 := \|\nabla \tilde{s}_{1h}\|^2 \ge \lambda_1$

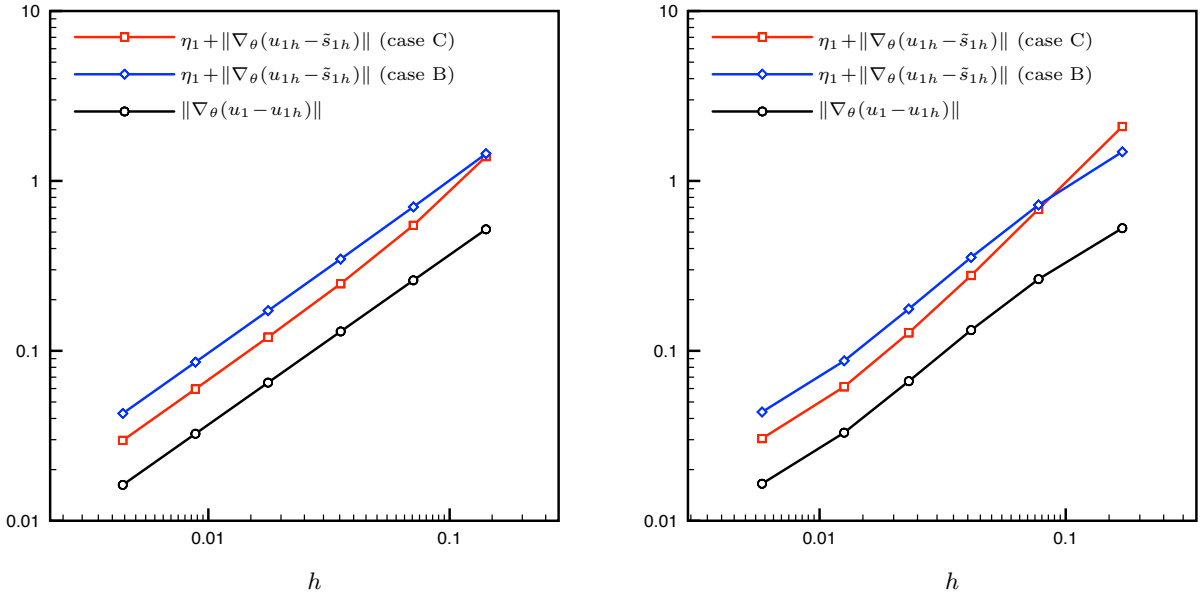

Figure 1: [Unit square, nonconforming method] Error in the eigenvector approximation and its upper bound for the choice $\underline{\lambda}_1 = 1.5\pi^2$, $\underline{\lambda}_2 = 4.5\pi^2$; sequence of structured (left) and unstructured but quasi-uniform (right) meshes

N	h	ndof	λ_1	λ_{1h}	$\|\nabla\tilde{s}_{1h}\|^2 - \eta_1^2$	$\|\nabla\tilde{s}_{1h}\|^2$	$E_{\lambda,\mathtt{rel}}$	$I^{\mathtt{ub}}_{u,\mathtt{eff}}$
10	0.1414	320	19.7392	19.6850	18.8966	19.8262	4.80e-02	2.68
20	0.0707	1 240	19.7392	19.7257	19.6495	19.7616	5.69e-03	2.11
40	0.0354	4 880	19.7392	19.7358	19.7246	19.7448	1.02e-03	1.91
80	0.0177	19 360	19.7392	19.7384	19.7361	19.7406	2.29e-04	1.85
160	0.0088	77 120	19.7392	19.7390	19.7385	19.7396	5.53e-05	1.83
320	0.0044	307 840	19.7392	19.7392	19.7390	19.7393	1.37e-05	1.83

Table 1: [Structured mesh, unit square, nonconforming method, case C] Lower and upper bounds of the exact eigenvalue λ_1, the relative eigenvalue error, and the eigenvector effectivity index; case $\underline{\lambda}_1 = 1.5\pi^2$, $\underline{\lambda}_2 = 4.5\pi^2$

following (6.15) as the auxiliary bounds in Theorems 6.1 and 6.4. The conditions (6.1) and (6.6b), (6.8b) respectively, turn out to be satisfied on all the meshes considered here.

Figure 1 illustrates the convergence of the energy error in the eigenfunction $\|\nabla_\theta(u_1 - u_{1h})\|$ and its upper bound $\eta_1 + \|\nabla_\theta(u_{1h} - \tilde{s}_{1h})\|$ of Theorem 6.4 for a sequence of uniform and structured meshes (left) and a sequence of unstructured quasi-uniform meshes (right). This test confirms that the convergence rate for the upper bound is the same as the one of the error in the approximation of the eigenvector, in accordance with Theorem 6.5, and this for both Cases B and C. As expected, Case C is sharper on finer meshes.

We present in Tables 1 and 2 precise values of the lower and upper bounds $\|\nabla\tilde{s}_{1h}\|^2 - \eta_1^2 \le \lambda_1 \le \|\nabla\tilde{s}_{1h}\|^2$ on the exact eigenvalue λ_1, the relative eigenvalue error, and the effectivity index of the eigenvector upper bound given respectively by

$$E_{\lambda,\mathtt{rel}} := 2\frac{\|\nabla\tilde{s}_{1h}\|^2 - (\|\nabla\tilde{s}_{1h}\|^2 - \eta_1^2)}{\|\nabla\tilde{s}_{1h}\|^2 + (\|\nabla\tilde{s}_{1h}\|^2 - \eta_1^2)} = \frac{2\,\eta_1^2}{2\,\|\nabla\tilde{s}_{1h}\|^2 - \eta_1^2}, \tag{8.1a}$$

$$I^{\mathtt{ub}}_{u,\mathtt{eff}} := \frac{\eta_1 + \|\nabla_\theta(u_{1h} - \tilde{s}_{1h})\|}{\|\nabla_\theta(u_1 - u_{1h})\|}. \tag{8.1b}$$

Note that (8.1a) is the eigenvalue upper bound minus the eigenvalue lower bound divided by the mean value of the upper and lower bounds, as in, e.g., [51] and the references therein. We observe rather convincing results.

N	h	ndof	λ_1	λ_{1h}	$\|\nabla\tilde{s}_{1h}\|^2-\eta_1^2$	$\|\nabla\tilde{s}_{1h}\|^2$	$E_{\lambda,\mathtt{rel}}$	$I^{\mathtt{ub}}_{u,\mathtt{eff}}$
10	0.1698	386	19.7392	19.6556	17.1037	19.8250	1.47e-01	3.97
20	0.0776	1 486	19.7392	19.7157	19.5482	19.7604	1.08e-02	2.58
40	0.0413	5 762	19.7392	19.7335	19.7167	19.7448	1.42e-03	2.10
80	0.0230	22 789	19.7392	19.7377	19.7353	19.7406	2.66e-04	1.93
160	0.0126	91 355	19.7392	19.7389	19.7384	19.7396	5.89e-05	1.86
320	0.0058	366 520	19.7392	19.7391	19.7390	19.7393	1.41e-05	1.84

Table 2: [Unstructured mesh, unit square, nonconforming method, case C] Lower and upper bounds of the exact eigenvalue λ_1, the relative eigenvalue error, and the eigenvector effectivity index; case $\underline{\lambda}_1 = 1.5\pi^2$, $\underline{\lambda}_2 = 4.5\pi^2$

8.1.2 L-shaped domain

We next consider the L-shaped domain $\Omega := (-1,1)^2 \setminus [0,1]\times[-1,0]$, where $\lambda_1 \approx 9.6397238440$ is known to high accuracy [60]. Including Ω into the square $\Omega^+ := (-1,1)^2$, cf. [17, Remark 5.4], we take $\underline{\lambda}_1 := \lambda_1(\Omega^+) = \pi^2/2 \approx 4.93$ (note that this is a very rough bound). We could similarly take $\underline{\lambda}_2 := \lambda_2(\Omega^+) = 5\pi^2/4 \approx 12.34$ (note that then $\lambda_1 < \underline{\lambda}_2 < \lambda_2 \approx 15.1973$). We, however, postpone this simplest choice to Section 8.2.2 below and choose here $\underline{\lambda}_2$ in Theorems 6.1 and 6.4 as the guaranteed lower bound computed on a coarse mesh of 6144 elements by the formula (6) of [51], $\underline{\lambda}_2 := 15.1753$ from Table 1 of [51].

We first consider a sequence of unstructured quasi-uniform meshes, with N elements partitioning the edges of Ω of length 2 and $N/2$ elements the edges of length 1. Figure 2 (left) illustrates the convergence of the eigenvector energy error $\|\nabla_\theta(u_1 - u_{1h})\|$ and its upper bound $\eta_1 + \|\nabla_\theta(u_{1h} - \tilde{s}_{1h})\|$. Details and eigenvalue convergence results are presented in Table 3. All the theoretical results are nicely confirmed.

We finally test adaptive refinement using the local character of the eigenvector estimator for each $K \in \mathcal{T}_h$ given by

$$\left(1 + 2(\lambda_{1h} + \|\nabla\tilde{s}_{1h}\|^2)\underline{\lambda}_2^{-1}\left(1 - \frac{\lambda_{1h}}{\underline{\lambda}_2}\right)^{-2}\right)\frac{1}{\|s_{1h}\|^2}$$
$$\left(\frac{\lambda_{1h}^2}{\underline{\lambda}_1}\|u_{1h} - s_{1h}\|_K^2 + \|\nabla s_{1h} + \boldsymbol{\sigma}_{1h}\|_K^2\right) + \|\nabla_\theta(u_{1h} - \tilde{s}_{1h})\|_K^2,$$

in case A and

$$\left(1 - \frac{\lambda_{1h}}{\underline{\lambda}_2}\right)^{-2}\left(1 - \frac{\overline{\alpha}_{1h}^2}{4}\right)^{-1}\frac{1}{\|s_{1h}\|^2}\left(\frac{\lambda_{1h}^2}{\underline{\lambda}_1}\|u_{1h} - s_{1h}\|_K^2 + \|\nabla s_{1h} + \boldsymbol{\sigma}_{1h}\|_K^2\right)$$
$$+ \|\nabla_\theta(u_{1h} - \tilde{s}_{1h})\|_K^2,$$

in case B of Theorems 6.1 and 6.4. We employ the Dörfler marking [33] with $\theta = 0.6$ and the newest vertex bisection mesh refinement. The same lower bounds $\underline{\lambda}_1 = \pi^2/2$ and $\underline{\lambda}_2 = 15.1753$ as for the uniform refinement have been used for the auxiliary bounds. Figure 2 (right) illustrates the error in the eigenvector and its bound using (6.16). The optimal convergence rate is indicated by dashed lines. The initial mesh is structured with 47 degrees of freedom and the conditions (6.1) and (6.6b) are both satisfied starting from 296 degrees of freedom. The transition from Case A to Case B in Theorem 6.4 is marked by a dotted line. Table 4 then presents more details of the adaptive procedure, which in particular leads to quite good effectivity indices.

8.2 Discontinuous Galerkin finite element method

In order to test the framework on another method, we have taken the symmetric version ($\theta = 1$) of the discontinuous Galerkin finite element method as presented in Section 7.2, using piecewise affine basis functions ($p = 1$) or piecewise quadratic basis functions ($p = 2$) and the penalty parameter $\nu = 10$.

8.2.1 Unit square

We consider again first the case of the unit square $\Omega = (0,1)^2$. The test case and the constants used are the same as presented in Section 8.1.1.

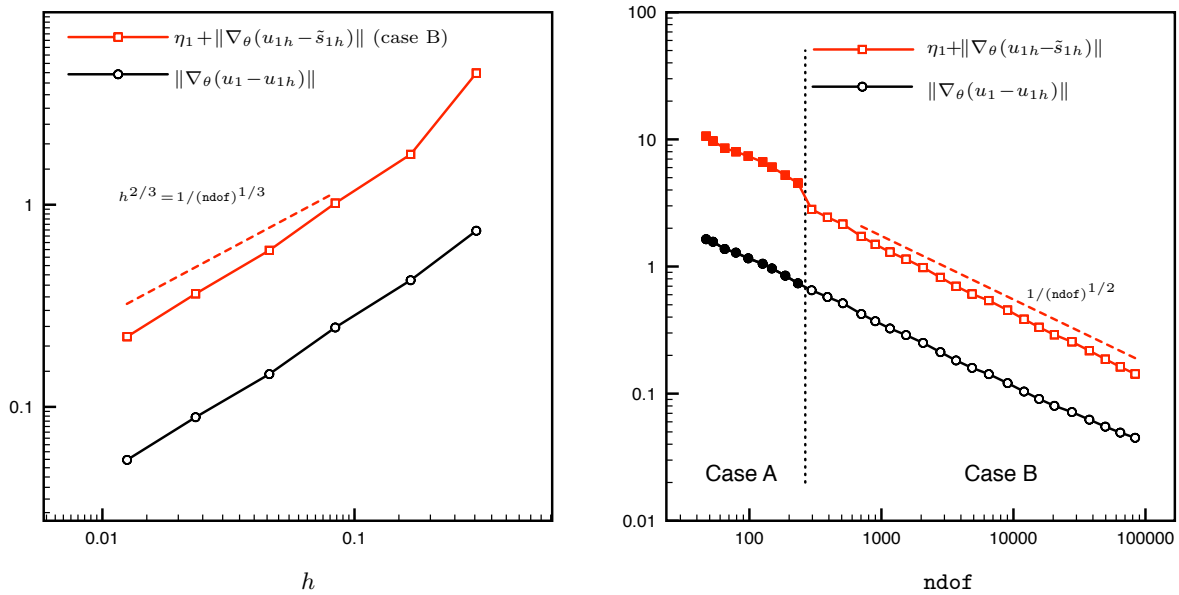

Figure 2: [Unstructured and adaptive mesh refinement, L-shaped domain, nonconforming method] Error in the eigenvector and its upper bound for a quasi-uniform refinement (left) and adaptive refinement (right); filled markers (case A), empty markers (case B)

N	h	ndof	λ_1	λ_{1h}	$\|\nabla\tilde{s}_{1h}\|^2 - \eta_1^2$	$\|\nabla\tilde{s}_{1h}\|^2$	$E_{\lambda,\texttt{rel}}$	$I^{\texttt{ub}}_{u,\texttt{eff}}$
10	0.3041	266	9.6397	9.2966	-4.1909	9.7861	–	6.02
20	0.1670	1 069	9.6397	9.5155	7.8895	9.6926	2.05e-01	4.19
40	0.0839	4 148	9.6397	9.5933	9.0782	9.6578	6.19e-02	4.12
80	0.0459	16 699	9.6397	9.6227	9.4514	9.6459	2.04e-02	4.09
160	0.0234	64 991	9.6397	9.6331	9.5703	9.6420	7.46e-03	4.08
320	0.0125	259 147	9.6397	9.6372	9.6138	9.6406	2.78e-03	4.07

Table 3: [Unstructured mesh, L-shaped domain, nonconforming method] Lower and upper bounds of the exact eigenvalue λ_1, the relative eigenvalue error, and the eigenvector effectivity index; case $\underline{\lambda}_1 = \pi^2/2$ and $\underline{\lambda}_2 = 15.1753$

Figure 3 illustrates the convergence of the energy error in the eigenfunction $\|\nabla_\theta(u_1 - u_{1h})\|$ and its guaranteed and computable a posteriori estimate $\eta_1 + \|\nabla_\theta(u_{1h} - \tilde{s}_{1h})\|$ of Theorem 6.4 for a sequence of uniform and structured meshes (left) and a sequence of unstructured quasi-uniform meshes (right). As the auxiliary eigenvalue lower bounds, we have taken here again $\underline{\lambda}_1 = 1.5\pi^2$ and $\underline{\lambda}_2 = 4.5\pi^2$. Tables 5–6 and 7–10 then give more details in Case C, also reporting the eigenvalue bounds of Theorems 6.1 and 6.3. In particular, for comparison, we include also much less precise choices $\underline{\lambda}_1 = 0.5\pi^2$ and $\underline{\lambda}_2 = 3\pi^2$. In the present Case C, the leading term stays unchanged, and the difference between the two tested pairs of $\underline{\lambda}_1$ and $\underline{\lambda}_2$ vanishes with mesh refinement. The results are rather sharp and confirm the theory nicely, in all tested settings.

8.2.2 L-shaped domain

We consider again as for the nonconforming method the L-shaped domain $\Omega := (-1,1)^2 \setminus [0,1] \times [-1,0]$ as a second test problem. Following Section 8.1.2, we consider three different choices of $\underline{\lambda}_1$ and $\underline{\lambda}_2$ in Theorems 6.1 and 6.4. Either $\underline{\lambda}_1 := \pi^2/2$ and $\underline{\lambda}_2 := 5\pi^2/4$ motivated by the simple inclusion of Ω into the square $\Omega^+ := (-1,1)^2$ (rough auxiliary bounds following [17, Remark 5.4]), or $\underline{\lambda}_1 := 9.6090$ and $\underline{\lambda}_2 := 15.1753$ (sharp auxiliary bounds numerically computed on a coarse mesh in Table 1 of [51]), or mixed accuracy auxiliary bounds $\underline{\lambda}_1 = \pi^2/2$ and $\underline{\lambda}_2 = 15.1753$.

Figure 4 (left) illustrates the convergence of the energy error $\|\nabla_\theta(u_1 - u_{1h})\|$ and its upper bound

Level	ndof	λ_1	λ_{1h}	$\|\nabla\tilde{s}_{1h}\|^2-\eta_1^2$	$\|\nabla\tilde{s}_{1h}\|^2$	$E_{\lambda,\mathtt{rel}}$	$I^{\mathtt{ub}}_{u,\mathtt{eff}}$
5	98	9.6397	8.9699	-29.6187	9.9072	–	6.36
10	296	9.6397	9.4403	4.8193	9.7445	6.76e-01	4.32
15	1 161	9.6397	9.5868	8.6628	9.6646	1.09e-01	3.99
20	4 860	9.6397	9.6275	9.4310	9.6457	2.25e-02	3.81
25	20 429	9.6397	9.6369	9.5925	9.6411	5.06e-03	3.62
30	83 472	9.6397	9.6390	9.6284	9.6401	1.21e-03	3.18

Table 4: [Adaptive mesh refinement, L-shaped domain, nonconforming method] Lower and upper bounds of the exact eigenvalue λ_1, the relative eigenvalue error, and the eigenvector effectivity index; case $\underline{\lambda}_1 = \pi^2/2$ and $\underline{\lambda}_2 = 15.1753$

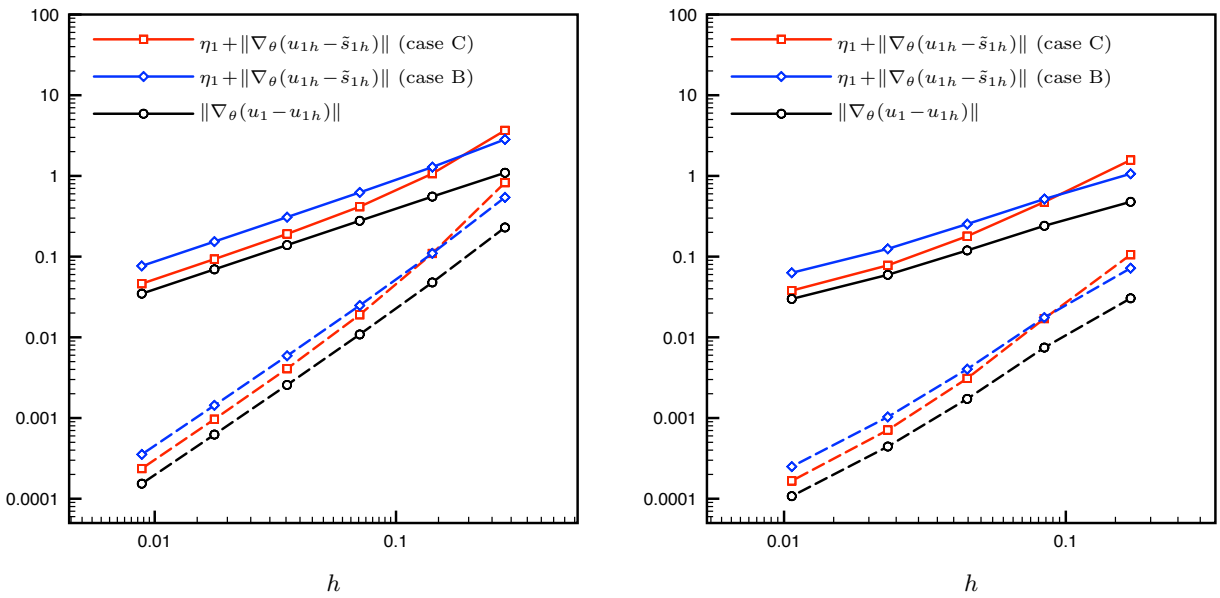

Figure 3: [Unit square, discontinuous Galerkin method] Error in the eigenvector approximation and its upper bound for the choice $\underline{\lambda}_1 = 1.5\pi^2$, $\underline{\lambda}_2 = 4.5\pi^2$; sequence of structured (left) and unstructured but quasi-uniform (right) meshes; $p = 1$ (full lines), $p = 2$ (dashed lines)

$\eta_1 + \|\nabla_\theta(u_{1h} - \tilde{s}_{1h})\|$ for the mixed accuracy auxiliary bounds $\underline{\lambda}_1 = \pi^2/2$ and $\underline{\lambda}_2 = 15.1753$. More details are presented in Tables 11–14. All the theoretical results of Theorems 6.1–6.5 appear nicely confirmed, with excellent effectivity indices. In particular, the eigenvector effectivity indices are slightly higher for $p = 2$ compared to $p = 1$ in Section 8.2.1, but often smaller here for $p = 2$ than for $p = 1$. In the present Case B, as expected from the theory, the two considered choices of $\underline{\lambda}_1$ and $\underline{\lambda}_2$ do not influence the order of convergence of our estimates, only the multiplicative constant. Consequently, the effectivity indices for the rough auxiliary bounds $\underline{\lambda}_1 = \pi^2/2$ and $\underline{\lambda}_2 = 5\pi^2/4$ are somewhat worse than those for the sharp auxiliary bounds $\underline{\lambda}_1 := 9.6090$ and $\underline{\lambda}_2 := 15.1753$, but the gap between them does not change with mesh refinement. Also, it seems from the comparison of Tables 11 and 12 for $p = 1$ versus Tables 13 and 14 for $p = 2$ that the higher polynomial degree is less impacted by the quality of the auxiliary bounds $\underline{\lambda}_1$ and $\underline{\lambda}_2$.

We finally test adaptive mesh refinement as outlined in Section 8.1.2. The initial mesh is structured with 47 degrees of freedom and the conditions (6.1) and (6.6b) are all satisfied starting from 591 degrees of freedom for $p = 1$. Figure 4 (right) illustrates the error in the eigenvector and its bound using (6.16). The optimal convergence rate is indicated by dashed lines. We observe improvement of the convergence rate in passing from uniform (Figure 4 (left)) to adaptive (Figure 4 (right)) mesh refinement. For polynomial degree $p = 1$, the convergence rate is improved from $1/(\mathtt{ndof})^{1/3}$ to $1/(\mathtt{ndof})^{1/2}$, whereas for polynomial degree $p = 2$, the convergence rate is improved from $1/(\mathtt{ndof})^{1/3}$ to $1/(\mathtt{ndof})$. It is to be noted therefrom that the rise of the polynomial degree from 1 to 2 only improves the rate for adaptive mesh refinement and not the uniform one, where it merely, as usually, decreases the quantitative prefactor. For adaptive

N	h	ndof	λ_1	λ_{1h}	$\|\nabla\tilde{s}_{1h}\|^2-\eta_1^2$	$\|\nabla\tilde{s}_{1h}\|^2$	$E_{\lambda,\mathtt{rel}}$	$I^{\mathtt{ub}}_{u,\mathtt{eff}}$
10	0.1414	600	19.7392	20.0333	19.1803	20.0101	4.23e-02	1.93
20	0.0707	2 400	19.7392	19.8169	19.6907	19.8099	6.03e-03	1.50
40	0.0354	9 600	19.7392	19.7591	19.7324	19.7572	1.26e-03	1.37
80	0.0177	38 400	19.7392	19.7442	19.7378	19.7438	2.99e-04	1.34
160	0.0088	153 600	19.7392	19.7405	19.7389	19.7403	7.39e-05	1.33

Table 5: [Structured mesh, unit square, discontinuous Galerkin method, case C, $p = 1$] Lower and upper bounds of the exact eigenvalue λ_1, the relative eigenvalue error, and the eigenvector effectivity index; intermediate accuracy auxiliary bounds $\underline{\lambda}_1 = 1.5\pi^2$, $\underline{\lambda}_2 = 4.5\pi^2$

N	h	ndof	λ_1	λ_{1h}	$\|\nabla\tilde{s}_{1h}\|^2-\eta_1^2$	$\|\nabla\tilde{s}_{1h}\|^2$	$E_{\lambda,\mathtt{rel}}$	$I^{\mathtt{ub}}_{u,\mathtt{eff}}$
10	0.1414	1 200	19.7392	19.7395	19.7343	19.7407	3.23e-04	2.29
20	0.0707	4 800	19.7392	19.7392	19.7391	19.7393	7.99e-06	1.76
40	0.0354	19 200	19.7392	19.7392	19.7392	19.7392	3.38e-07	1.59
80	0.0177	76 800	19.7392	19.7392	19.7392	19.7392	1.86e-08	1.55
160	0.0088	307 200	19.7392	19.7392	19.7392	19.7392	1.12e-09	1.54

Table 6: [Structured mesh, unit square, discontinuous Galerkin method, case C, $p = 2$] Lower and upper bounds of the exact eigenvalue λ_1, the relative eigenvalue error, and the eigenvector effectivity index; intermediate accuracy auxiliary bounds $\underline{\lambda}_1 = 1.5\pi^2$, $\underline{\lambda}_2 = 4.5\pi^2$

mesh refinement, the difference is rather spectacular: $p = 1$ achieves roughly 0.1 energy error accuracy for a little less than 100.000 degrees of freedom, whereas $p = 2$ yields 0.01 accuracy for a little more than 10.000 degrees of freedom. Tables 15 and 16 then present more details.

9 Concluding remarks

The motivation of the present paper was to develop a general theory of eigenvalue and eigenvector a posteriori error estimates, enabling to take into account basically any numerical method. This in particular means that we need to admit the violation of the constraints $u_{ih} \in H^1_0(\Omega)$, $\|u_{ih}\| = 1$, $\|\nabla_\theta u_{ih}\|^2 = \lambda_{ih}$, and $\lambda_{ih} \geq \lambda_i$. Our bounds from Section 6 achieve this and we have seen in Section 7 that three common nonconforming numerical methods fit perfectly the framework. Moreover, typically, not all the above constraints are violated. Then parts of the results of Section 6 simplify importantly.

We have focused here for simplicity on the treatment of the case where the underlying algebraic eigenvalue solvers are exact, so that the present Assumption 3.1 can be satisfied. The framework is, however, built rich enough to take into account inexact solvers, following [37, 57] and the references therein, as we have demonstrated it in [17]. The resulting estimates are then valid on an arbitrary eigenvalue iterative solver step, enable to distinguish the different error components, and yield (local) adaptive stopping criteria. A preliminary example in the context of the Gross–Pitaevskii nonlinear eigenvalue problem is given in [16].

The approximation polynomial degree p was considered fixed here and we have only treated the case of matching simplicial meshes. Extension to variable polynomial degree and nonmatching simplicial and quadrilateral meshes is straightforward following [32], where also *hp* (mesh and polynomial degree) adaptive refinement strategies are developed. It should be rather easy to generalize them to the present eigenvalue setting.

Acknowledgements

We would like to thank Frédéric Hecht (Laboratoire Jacques-Louis Lions, Sorbonne Université) for his kind help with our higher-order implementation in the FreeFem++ code [42, 43].

N	h	ndof	λ_1	λ_{1h}	$\|\nabla\tilde{s}_{1h}\|^2-\eta_1^2$	$\|\nabla\tilde{s}_{1h}\|^2$	$E_{\lambda,\mathtt{rel}}$	$I^{\mathtt{ub}}_{u,\mathtt{eff}}$
10	0.1698	708	19.7392	19.9432	17.8299	19.9511	1.12e-01	3.29
20	0.0839	2 820	19.7392	19.7930	19.6125	19.7944	9.24e-03	1.97
40	0.0447	11 388	19.7392	19.7525	19.7284	19.7529	1.24e-03	1.50
80	0.0233	44 868	19.7392	19.7425	19.7381	19.7426	2.31e-04	1.31
160	0.0106	181 428	19.7392	19.7400	19.7390	19.7401	5.32e-05	1.27

Table 7: [Unstructured mesh, unit square, discontinuous Galerkin method, case C, $p = 1$] Lower and upper bounds of the exact eigenvalue λ_1, the relative eigenvalue error, and the eigenvector effectivity index; intermediate accuracy auxiliary bounds $\underline{\lambda}_1 = 1.5\pi^2$, $\underline{\lambda}_2 = 4.5\pi^2$

N	h	ndof	λ_1	λ_{1h}	$\|\nabla\tilde{s}_{1h}\|^2-\eta_1^2$	$\|\nabla\tilde{s}_{1h}\|^2$	$E_{\lambda,\mathtt{rel}}$	$I^{\mathtt{ub}}_{u,\mathtt{eff}}$
10	0.1698	708	19.7392	19.9432	13.4605	19.9511	3.89e-01	5.58
20	0.0839	2 820	19.7392	19.7930	19.3593	19.7944	2.22e-02	2.94
40	0.0447	11 388	19.7392	19.7525	19.7112	19.7529	2.11e-03	1.90
80	0.0233	44 868	19.7392	19.7425	19.7369	19.7426	2.88e-04	1.44
160	0.0106	181 428	19.7392	19.7400	19.7390	19.7401	5.64e-05	1.30

Table 8: [Unstructured mesh, unit square, discontinuous Galerkin method, case C, $p = 1$] Lower and upper bounds of the exact eigenvalue λ_1, the relative eigenvalue error, and the eigenvector effectivity index; rough auxiliary bounds $\underline{\lambda}_1 = 0.5\pi^2$, $\underline{\lambda}_2 = 3\pi^2$

Appendix

The current analysis was presented for the Laplace operator of (1.1). The generic equivalences can, however, be extended to a larger class of operators that we show in part A of this appendix, for a conforming approximation. We next complement in part B the estimate of Theorem 6.3 by a further possible improvement of the first eigenvalue upper bound.

A Extension to a generic operator

We formulate here the results of [17, Theorems 3.4 and 3.5] for conforming approximations and any bounded-below self-adjoint operator with compact resolvent, see, e.g., Helffer [44]. This comprises for example the operator $A := -\Delta + w$ with domain $D(A) := \{v \in H^1_0(\Omega); \Delta v \in L^2(\Omega)\}$, which is self-adjoint on $L^2(\Omega)$ whenever $w \in L^\infty(\Omega)$. It appears that only the operator considered $(-\Delta)$ and the norms $(\|\cdot\|, \|\nabla\cdot\|$, and $\|\cdot\|_{-1})$ need to be changed.

Let $\mathcal{H}$ be a separable Hilbert space endowed with a scalar product denoted by $(\cdot,\cdot)_{\mathcal{H}}$. Now let A be a bounded-below self-adjoint operator on $\mathcal{H}$ with domain $D(A)$ and compact resolvent. There exists a non-decreasing sequence of real numbers $(\lambda_k)_{k\geq 1}$ such that $\lambda_k \to \infty$ and an orthonormal basis $(u_k)_{k\geq 1}$ of $\mathcal{H}$ consisting of vectors of $D(A)$ such that

$$\forall k \geq 1, \quad A\,u_k = \lambda_k u_k.$$

Making the additional assumption that the k-th eigenvalue of A is simple, that is $\lambda_{k-1} < \lambda_k < \lambda_{k+1}$, the k-th eigenvector is unique up to the sign. Up to shifting the operator A by a constant $c \in \mathbb{R}^+$ such that $c + A$ is a positive definite operator, we can suppose that A is a positive definite operator, in which case $(\lambda_k)_{k\geq 1}$ is a sequence of positive numbers. This enables to define an operator $A^{\frac{1}{2}}$ analogous to the operator $|\nabla|$ in the previous case (recall that $\||\nabla v|\| = \|\nabla v\|$ for $v \in H^1(\Omega)$) by its domain

$$D(A^{\frac{1}{2}}) := \left\{ v \in \mathcal{H}; \quad \sum_{k\geq 1} \lambda_k |(v, u_k)_{\mathcal{H}}|^2 < +\infty \right\}$$

and its expression

$$A^{\frac{1}{2}} : v \in D(A^{\frac{1}{2}}) \mapsto \sum_{k\geq 1} \sqrt{\lambda_k}(v, u_k)_{\mathcal{H}} u_k.$$

N	h	ndof	λ_1	λ_{1h}	$\|\nabla\tilde{s}_{1h}\|^2-\eta_1^2$	$\|\nabla\tilde{s}_{1h}\|^2$	$E_{\lambda,\mathtt{rel}}$	$I^{\mathtt{ub}}_{u,\mathtt{eff}}$
10	0.1698	1 416	19.7392	19.7394	19.7320	19.7399	3.98e-04	3.47
20	0.0839	5 640	19.7392	19.7392	19.7391	19.7393	8.24e-06	2.29
40	0.0447	22 776	19.7392	19.7392	19.7392	19.7392	2.34e-07	1.79
80	0.0233	89 736	19.7392	19.7392	19.7392	19.7392	1.14e-08	1.60
160	0.0106	362 856	19.7392	19.7392	19.7392	19.7392	5.97e-10	1.55

Table 9: [Unstructured mesh, unit square, discontinuous Galerkin method, case C, $p = 2$] Lower and upper bounds of the exact eigenvalue λ_1, the relative eigenvalue error, and the eigenvector effectivity index; intermediate accuracy auxiliary bounds $\underline{\lambda}_1 = 1.5\pi^2$, $\underline{\lambda}_2 = 4.5\pi^2$

N	h	ndof	λ_1	λ_{1h}	$\|\nabla\tilde{s}_{1h}\|^2-\eta_1^2$	$\|\nabla\tilde{s}_{1h}\|^2$	$E_{\lambda,\mathtt{rel}}$	$I^{\mathtt{ub}}_{u,\mathtt{eff}}$
10	0.1698	1 416	19.7392	19.7394	19.7129	19.7399	1.37e-03	5.96
20	0.0839	5 640	19.7392	19.7392	19.7388	19.7393	2.32e-05	3.44
40	0.0447	22 776	19.7392	19.7392	19.7392	19.7392	4.53e-07	2.28
80	0.0233	89 736	19.7392	19.7392	19.7392	19.7392	1.53e-08	1.77
160	0.0106	362 856	19.7392	19.7392	19.7392	19.7392	6.50e-10	1.59

Table 10: [Unstructured mesh, unit square, discontinuous Galerkin method, case C, $p = 2$] Lower and upper bounds of the exact eigenvalue λ_1, the relative eigenvalue error, and the eigenvector effectivity index; rough auxiliary bounds $\underline{\lambda}_1 = 0.5\pi^2$, $\underline{\lambda}_2 = 3\pi^2$

Replace now $-\Delta$ by A; for the norms, the scalar product $(\cdot,\cdot)_{\mathcal{H}}$ of the Hilbert space $\mathcal{H}$ substitutes the L^2 scalar product $(\cdot,\cdot)$, and naturally the norm of $\|\cdot\|_{\mathcal{H}}$ replaces the L^2-norm $\|\cdot\|$. The energy norm $\|\nabla\cdot\|$ is changed into $\|A^{\frac{1}{2}}\cdot\|_{\mathcal{H}}$, and the duality pairing $\langle\cdot,\cdot\rangle_{V',V}$ becomes $\langle\cdot,\cdot\rangle_{D(A^{\frac{1}{2}})',D(A^{\frac{1}{2}})}$.

Let $(w_i,\lambda_{ih}) \in D(A^{\frac{1}{2}}) \times \mathbb{R}^+$ with $\|w_i\|_{\mathcal{H}} = 1$ and $(w_i,\chi_i)_{\mathcal{H}} > 0$ be given, for $\chi_i \in \mathcal{H}$, $i \geq 1$ fixed. Its residual $\mathrm{Res}_\theta(w_i,\lambda_{ih}) \in D(A^{\frac{1}{2}})'$ is now defined by

$$\langle \mathrm{Res}_\theta(w_i,\lambda_{ih}), v\rangle_{D(A^{\frac{1}{2}})',D(A^{\frac{1}{2}})} := \lambda_{ih}(w_i,v)_{\mathcal{H}} - (A^{\frac{1}{2}}w_i, A^{\frac{1}{2}}v)_{\mathcal{H}} \qquad \forall v \in D(A^{\frac{1}{2}}),$$

with the dual norm

$$\|\mathrm{Res}_\theta(w_i,\lambda_{ih})\|_{D(A^{\frac{1}{2}})'} := \sup_{v\in D(A^{\frac{1}{2}}),\, \|A^{\frac{1}{2}}v\|_{\mathcal{H}}=1} \langle \mathrm{Res}_\theta(w_i,\lambda_{ih}), v\rangle_{D(A^{\frac{1}{2}})',D(A^{\frac{1}{2}})}.$$

The Riesz representation of the residual $\mathscr{r}_{w_i} \in D(A^{\frac{1}{2}})$ is given by

$$(A^{\frac{1}{2}}\mathscr{r}_{w_i}, A^{\frac{1}{2}}v)_{\mathcal{H}} = \langle \mathrm{Res}_\theta(w_i,\lambda_{ih}), v\rangle_{D(A^{\frac{1}{2}})',D(A^{\frac{1}{2}})} \qquad \forall v \in D(A^{\frac{1}{2}}).$$

Let

$$\lambda_{i-1} < \lambda_{ih} \quad \text{when } i > 1, \quad \lambda_{ih} < \lambda_{i+1}, \tag{A.1}$$

and

$$\alpha_{ih} := \sqrt{2}C_{ih}^{-\frac{1}{2}}\|\mathscr{r}_{w_i}\|_{\mathcal{H}} \leq \|\chi_i\|_{\mathcal{H}}^{-1}(w_i,\chi_i)_{\mathcal{H}}, \tag{A.2}$$

where

$$C_{ih} := \min\left\{\left(1-\frac{\lambda_{ih}}{\lambda_{i-1}}\right)^2, \left(1-\frac{\lambda_{ih}}{\lambda_{i+1}}\right)^2\right\}.$$

The generalizations of [17, Theorems 3.4 and 3.5] then read:

Theorem A.1 (Eigenvalue bounds). *Let $(w_i,\lambda_{ih}) \in D(A^{\frac{1}{2}}) \times \mathbb{R}^+$ with $\|w_i\|_{\mathcal{H}} = 1$ and $(w_i,\chi_i)_{\mathcal{H}} > 0$, $i \geq 1$. Let assumptions (A.1) and (A.2) be satisfied. Then*

$$\|A^{\frac{1}{2}}(u_i - w_i)\|_{\mathcal{H}}^2 - \lambda_i\alpha_{ih}^2 \leq \|A^{\frac{1}{2}}w_i\|_{\mathcal{H}}^2 - \lambda_i \leq \|A^{\frac{1}{2}}(u_i - w_i)\|_{\mathcal{H}}^2. \tag{A.3a}$$

If, moreover $\alpha_{1h} \leq \sqrt{2}$, then, for $i = 1$,

$$\frac{1}{2}\left(1-\frac{\lambda_1}{\lambda_2}\right)\left(1-\frac{\alpha_{1h}^2}{4}\right)\|A^{\frac{1}{2}}(u_1 - w_1)\|_{\mathcal{H}}^2 \leq \|A^{\frac{1}{2}}w_1\|_{\mathcal{H}}^2 - \lambda_1. \tag{A.3b}$$

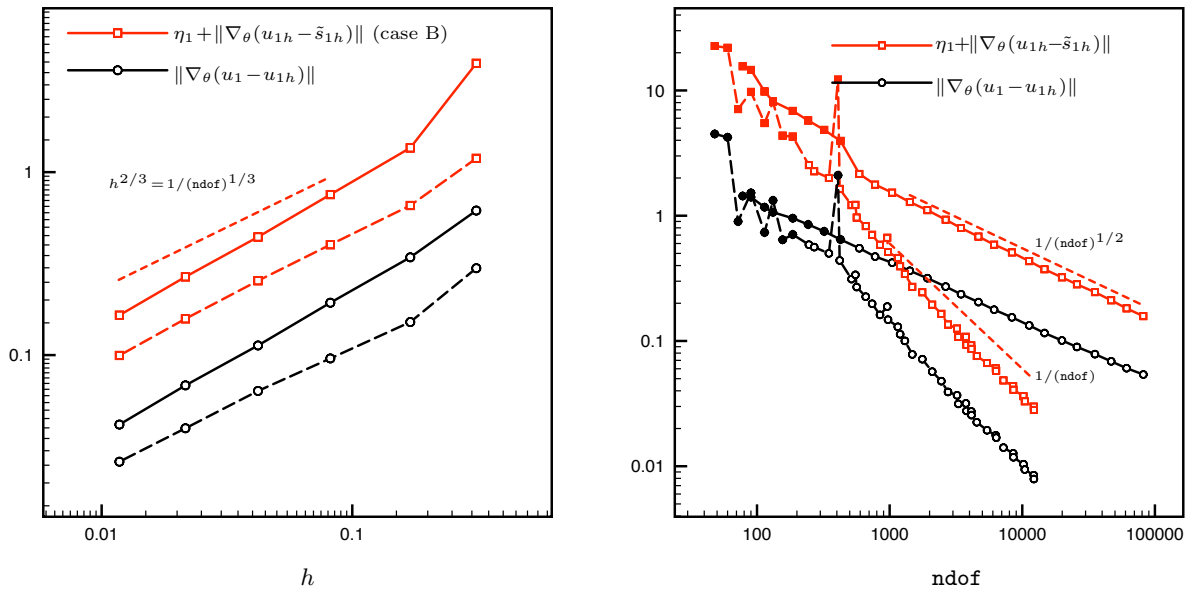

Figure 4: [Unstructured and adaptive mesh refinement, L-shaped domain, discontinuous Galerkin method] Error in the eigenvector and its upper bound for a quasi-uniform refinement (left) and adaptive refinement (right); $p = 1$ (full lines), $p = 2$ (dashed lines); filled markers (case A), empty markers (case B)

N	h	ndof	λ_1	λ_{1h}	$\|\nabla\tilde{s}_{1h}\|^2 - \eta_1^2$	$\|\nabla\tilde{s}_{1h}\|^2$	$E_{\lambda,\texttt{rel}}$	$I^{\texttt{ub}}_{u,\texttt{eff}}$
10	0.3124	504	9.6397	9.8824	-3.2766	9.9823	–	6.38
20	0.1703	1 986	9.6397	9.7050	8.3517	9.7447	1.54e-01	3.97
40	0.0817	8 070	9.6397	9.6579	9.2527	9.6728	4.44e-02	3.90
80	0.0421	33 438	9.6397	9.6447	9.5098	9.6507	1.47e-02	3.92
160	0.0216	130 080	9.6397	9.6413	9.5926	9.6436	5.31e-03	3.92
320	0.0118	516 876	9.6397	9.6402	9.6221	9.6412	1.98e-03	3.96

Table 11: [Unstructured mesh, L-shaped domain, discontinuous Galerkin method, $p = 1$] Lower and upper bounds of the exact eigenvalue λ_1, the relative eigenvalue error, and the eigenvector effectivity index; sharp auxiliary bounds $\underline{\lambda}_1 = 9.6090$ and $\underline{\lambda}_2 = 15.1753$

Let

$$\overline{C}_{ih} := 1 \text{ if } i = 1, \quad \overline{C}_{ih} := \max\left\{\left(\frac{\lambda_{ih}}{\lambda_1} - 1\right)^2, 1\right\} \text{ if } i > 1$$

and

$$\gamma_{ih} := \begin{cases} \|A^{\frac{1}{2}}(u_i - w_i)\|^2_{\mathcal{H}} & \text{if } \lambda_i \le \|A^{\frac{1}{2}} w_i\|^2_{\mathcal{H}} \text{ is known to hold,} \\ \max\{\|A^{\frac{1}{2}}(u_i - w_i)\|^2_{\mathcal{H}}, \lambda_i \alpha^2_{ih}\} & \text{otherwise.} \end{cases} \tag{A.4}$$

Then we also have:

Theorem A.2 (Eigenvector bounds)**.** *Let the assumptions of Theorem A.1 be satisfied. Then*

$$\|A^{\frac{1}{2}}(u_i - w_i)\|^2_{\mathcal{H}} \le \|\mathrm{Res}_\theta(w_i, \lambda_{ih})\|^2_{D(A^{\frac{1}{2}})'} + (\lambda_{ih} + \lambda_i)\alpha^2_{ih}, \tag{A.5a}$$

$$\|\mathrm{Res}_\theta(w_i, \lambda_{ih})\|^2_{D(A^{\frac{1}{2}})'} \le \frac{\left(\left|\lambda_{ih} - \|A^{\frac{1}{2}} w_i\|^2_{\mathcal{H}}\right| + \gamma_{ih}\right)^2}{\lambda_i} + \overline{C}_{ih}\|A^{\frac{1}{2}}(u_i - w_i)\|^2_{\mathcal{H}}. \tag{A.5b}$$

If, moreover $\alpha^2_{ih} \le 2\frac{\lambda_1}{\lambda_i}$*, then*

$$\|A^{\frac{1}{2}}(u_i - w_i)\|^2_{\mathcal{H}} \le C_{ih}^{-1}\left(1 - \frac{\lambda_i}{\lambda_1}\frac{\alpha^2_{ih}}{4}\right)^{-1}\|\mathrm{Res}_\theta(w_i, \lambda_{ih})\|^2_{D(A^{\frac{1}{2}})'}.$$

N	h	ndof	λ_1	λ_{1h}	$\|\nabla\tilde{s}_{1h}\|^2-\eta_1^2$	$\|\nabla\tilde{s}_{1h}\|^2$	$E_{\lambda,\mathtt{rel}}$	$I^{\mathtt{ub}}_{u,\mathtt{eff}}$
10	0.3124	504	9.6397	9.8824	-41.1501	9.9823	–	12.07
20	0.1703	1 986	9.6397	9.7050	-2.7955	9.7447	–	10.87
40	0.0817	8 070	9.6397	9.6579	8.4329	9.6728	1.37e-01	6.31
80	0.0421	33 438	9.6397	9.6447	9.2496	9.6507	4.24e-02	6.20
160	0.0216	130 080	9.6397	9.6413	9.5001	9.6436	1.50e-02	6.16
320	0.0118	516 876	9.6397	9.6402	9.5880	9.6412	5.53e-03	6.18

Table 12: [Unstructured mesh, L-shaped domain, discontinuous Galerkin method, $p=1$] Lower and upper bounds of the exact eigenvalue λ_1, the relative eigenvalue error, and the eigenvector effectivity index; rough auxiliary bounds $\underline{\lambda}_1=\pi^2/2$ and $\underline{\lambda}_2=5\pi^2/4$

N	h	ndof	λ_1	λ_{1h}	$\|\nabla\tilde{s}_{1h}\|^2-\eta_1^2$	$\|\nabla\tilde{s}_{1h}\|^2$	$E_{\lambda,\mathtt{rel}}$	$I^{\mathtt{ub}}_{u,\mathtt{eff}}$
10	0.3124	1 008	9.6397	9.6106	8.8410	9.6862	9.12e-02	3.99
20	0.1703	3 972	9.6397	9.6267	9.4042	9.6533	2.61e-02	4.34
40	0.0817	16 140	9.6397	9.6347	9.5535	9.6452	9.55e-03	4.19
80	0.0421	66 876	9.6397	9.6376	9.6056	9.6420	3.79e-03	4.00
160	0.0216	260 160	9.6397	9.6389	9.6267	9.6406	1.44e-03	3.97

Table 13: [Unstructured mesh, L-shaped domain, discontinuous Galerkin method, $p=2$] Lower and upper bounds of the exact eigenvalue λ_1, the relative eigenvalue error, and the eigenvector effectivity index; sharp auxiliary bounds $\underline{\lambda}_1=9.6090$ and $\underline{\lambda}_2=15.1753$

B Further improvement of the first eigenvalue upper bound

In [17, Theorem 5.2], a further improvement of the eigenvalue upper bounds of type of Theorem 6.3 was possible. We now extend it to the present setting, for the first eigenvalue.

We first need to generalize the conforming local residual lifting from [17, Section 4.3] to the present setting. Let for each vertex $\mathbf{a}\in\mathcal{V}_h$, $X_h^{\mathbf{a}}$ be an arbitrary finite-dimensional subspace of the space $H^1_*(\omega_{\mathbf{a}})$ defined in (4.1). Typically, $X_h^{\mathbf{a}}:=\mathbb{P}_{p+1}(\mathcal{T}_{\mathbf{a}})\cap H^1_*(\omega_{\mathbf{a}})$, similarly as for $W_h^{\mathbf{a}}$ in Section 3.2. We will now solve *homogeneous local Neumann* (Neumann–Dirichlet close to the boundary) *problems* on the patches $\omega_{\mathbf{a}}$ via conforming primal counterparts of problems (3.3a):

Definition B.1 (Conforming local Neumann problems)**.** *For each $\mathbf{a}\in\mathcal{V}_h$, define $r_{1h}^{\mathbf{a}}\in X_h^{\mathbf{a}}$ by*

$$(\nabla r_{1h}^{\mathbf{a}},\nabla v_h)_{\omega_{\mathbf{a}}}=\langle\mathrm{Res}_\theta(s_{1h},\lambda_{1h}),\psi_{\mathbf{a}}v_h\rangle_{V',V}\qquad\forall v_h\in X_h^{\mathbf{a}}. \tag{B.1}$$

Then set

$$r_{1h}:=\sum_{\mathbf{a}\in\mathcal{V}_h}\psi_{\mathbf{a}}r_{1h}^{\mathbf{a}}\in V.$$

The functions $r_{1h}^{\mathbf{a}}$ are discrete Riesz representations of the local residual of the pair (s_{1h},λ_{1h}) with hat-weighted test functions. Note that the right-hand side in (B.1) does not necessarily satisfy the usually required Neumann compatibility condition $(\psi_{\mathbf{a}}\lambda_{1h}s_{1h}-\nabla s_{1h}\cdot\nabla\psi_{\mathbf{a}},1)_{\omega_{\mathbf{a}}}=0$ for $\mathbf{a}\in\mathcal{V}_h^{\mathrm{int}}$, so that (B.1) cannot hold for a constant function $v_h=1$ on $\omega_{\mathbf{a}}$. Assumption 3.1 is in particular not required for s_{1h}; this does not influence the existence and uniqueness of $r_{1h}^{\mathbf{a}}$ (the system matrix in (B.1) is regular). Note also that $r_{1h}^{\mathbf{a}}\notin V$ (when extended by zero outside of $\omega_{\mathbf{a}}$) but $\psi_{\mathbf{a}}r_{1h}^{\mathbf{a}}\in H^1_0(\omega_{\mathbf{a}})$, whence the sum r_{1h} belongs to V. For this construction, we have:

Lemma B.2 (Lower dual residual bound)**.** *Let $(u_{1h},\lambda_{1h})\in\mathbb{P}_p(\mathcal{T}_h)\times\mathbb{R}^+$ be arbitrary. Construct s_{1h} by Definition 3.3 and r_{1h} by Definition B.1. Then*

$$\frac{\langle\mathrm{Res}_\theta(s_{1h},\lambda_{1h}),r_{1h}\rangle_{V',V}}{\|\nabla r_{1h}\|}\le\|\mathrm{Res}_\theta(s_{1h},\lambda_{1h})\|_{-1}.$$

Proof. The proof is trivial from (2.7b) and from the fact that $r_{1h}\in V$ for Definition B.1. Importantly, this bound is positive, see [57, proof of Theorem 2]. □

Equipped with these tools, we can now hopefully improve the upper bound (6.15) in Theorem 6.3 (we actually only mimic the Case B of Theorem 6.1, the other cases can be treated similarly).

N	h	ndof	λ_1	λ_{1h}	$\|\nabla\tilde{s}_{1h}\|^2-\eta_1^2$	$\|\nabla\tilde{s}_{1h}\|^2$	$E_{\lambda,\mathtt{rel}}$	$I^{\mathtt{ub}}_{u,\mathtt{eff}}$
10	0.3124	1 008	9.6397	9.6106	6.9318	9.6862	3.32e-01	6.47
20	0.1703	3 972	9.6397	9.6267	8.9126	9.6533	7.98e-02	6.72
40	0.0817	16 140	9.6397	9.6347	9.3819	9.6452	2.77e-02	6.38
80	0.0421	66 876	9.6397	9.6376	9.5390	9.6420	1.07e-02	6.05
160	0.0216	260 160	9.6397	9.6389	9.6016	9.6406	4.06e-03	5.97

Table 14: [Unstructured mesh, L-shaped domain, discontinuous Galerkin method, $p=2$] Lower and upper bounds of the exact eigenvalue λ_1, the relative eigenvalue error, and the eigenvector effectivity index; rough auxiliary bounds $\underline{\lambda}_1=\pi^2/2$ and $\underline{\lambda}_2=5\pi^2/4$

Level	ndof	λ_1	λ_{1h}	$\|\nabla\tilde{s}_{1h}\|^2-\eta_1^2$	$\|\nabla\tilde{s}_{1h}\|^2$	$E_{\lambda,\mathtt{rel}}$	$I^{\mathtt{ub}}_{u,\mathtt{eff}}$
5	186	9.6397	10.2136	-30.6026	10.3629	–	7.19
10	777	9.6397	9.8154	7.2388	9.8388	3.04e-01	3.75
15	3 453	9.6397	9.6865	9.1572	9.6902	5.66e-02	3.38
20	14 706	9.6397	9.6509	9.5335	9.6517	1.23e-02	3.23
25	61 137	9.6397	9.6425	9.6144	9.6426	2.93e-03	3.00

Table 15: [Adaptive mesh refinement, L-shaped domain, discontinuous Galerkin method, $p=1$] Lower and upper bounds of the exact eigenvalue λ_1, the relative eigenvalue error, and the eigenvector effectivity index; mixed accuracy auxiliary bounds $\underline{\lambda}_1=\pi^2/2$ and $\underline{\lambda}_2=15.1753$

Proposition B.3 (Possible improvement of the first eigenvalue upper bound)**.** *Let $\underline{\lambda}_1,\underline{\lambda}_2$ be as in Theorem 6.1. Let $(u_{1h},\lambda_{1h})\in\mathbb{P}_p(\mathcal{T}_h)\times\mathbb{R}^+$, $p\geq 1$, be arbitrary. Let s_{1h} be constructed following Definition 3.3 and r_{1h} following Definition B.1. Let $(s_{1h},\chi_1)>0$ and*

$$\begin{aligned}\overline{\alpha}_{1h}&:=\sqrt{2}\left(1-\frac{\lambda_{1h}}{\underline{\lambda}_2}\right)^{-1}\underline{\lambda}_2^{-\frac{1}{2}}\frac{1}{\|s_{1h}\|}\left(\frac{\lambda_{1h}}{\sqrt{\underline{\lambda}_1}}\|u_{1h}-s_{1h}\|+\|\nabla s_{1h}+\boldsymbol{\sigma}_{1h}\|\right)\\&\leq\min\left\{\sqrt{2},\|\chi_1\|^{-1}(\tilde{s}_{1h},\chi_1)\right\},\end{aligned}$$

with $\tilde{s}_{1h}:=\frac{s_{1h}}{\|s_{1h}\|}$. Then

$$\lambda_1\leq\|\nabla\tilde{s}_{1h}\|^2-\tilde{\eta}_1,$$

where

$$\begin{aligned}\tilde{\eta}_1&:=\max\left\{\frac{1}{4}\left(1-\frac{\|\nabla\tilde{s}_{1h}\|^2}{\underline{\lambda}_2}\right)\left(1-\frac{\overline{\alpha}_{1h}^2}{4}\right)\left(\sqrt{d_h}-\left(\underline{\lambda}_1+2\left|\lambda_{1h}-\|\nabla\tilde{s}_{1h}\|^2\right|\right)\right),0\right\},\\d_h&:=\underline{\lambda}_1^2+4\underline{\lambda}_1\frac{\langle\mathrm{Res}_\theta(\tilde{s}_{1h},\lambda_{1h}),r_{1h}\rangle_{V',V}^2}{\|\nabla r_{1h}\|^2}+4\underline{\lambda}_1\left|\lambda_{1h}-\|\nabla\tilde{s}_{1h}\|^2\right|.\end{aligned}$$

Proof. Note first that all the assumptions of [17, Theorems 3.4 and 3.5] are satisfied. We start by the second bound in [17, Theorem 3.4] which immediately implies, using $\underline{\lambda}_1\leq\lambda_1$, $\underline{\lambda}_2\leq\lambda_2$, and $\lambda_1\leq\|\nabla\tilde{s}_{1h}\|$,

$$\lambda_1\leq\|\nabla\tilde{s}_{1h}\|^2-\frac{1}{2}\left(1-\frac{\|\nabla\tilde{s}_{1h}\|^2}{\underline{\lambda}_2}\right)\left(1-\frac{\overline{\alpha}_{1h}^2}{4}\right)\|\nabla(u_1-\tilde{s}_{1h})\|^2.$$

Similarly, the second bound in [17, Theorem 3.5] now takes the form

$$\|\mathrm{Res}_\theta(\tilde{s}_{1h},\lambda_{1h})\|_{-1}^2\leq\frac{\left(\left|\lambda_{1h}-\|\nabla\tilde{s}_{1h}\|^2\right|+\|\nabla\left(u_1-\tilde{s}_{1h}\right)\|^2\right)^2}{\lambda_1}+\|\nabla(u_1-\tilde{s}_{1h})\|^2.$$

Denote $l_h:=\left|\lambda_{1h}-\|\nabla\tilde{s}_{1h}\|^2\right|$, $R_h:=\langle\mathrm{Res}_\theta(\tilde{s}_{1h},\lambda_{1h}),r_{1h}\rangle_{V',V}^2/\|\nabla r_{1h}\|^2$, as well as $e_h:=\|\nabla\left(u_1-\tilde{s}_{1h}\right)\|^2$. Combined with Lemma B.2 and $0<\underline{\lambda}_1\leq\lambda_1$, this last inequality implies

$$e_h^2+e_h\left(\underline{\lambda}_1+2l_h\right)-\left(\underline{\lambda}_1R_h-l_h^2\right)\geq 0.$$

Level	ndof	λ_1	λ_{1h}	$\|\nabla\tilde{s}_{1h}\|^2 - \eta_1^2$	$\|\nabla\tilde{s}_{1h}\|^2$	$E_{\lambda,\mathtt{rel}}$	$I_{u,\mathtt{eff}}^{\mathtt{ub}}$
5	114	9.6397	9.4488	-13.0515	9.9443	–	7.47
10	270	9.6397	9.5727	6.4534	9.7848	4.10e-01	4.03
15	552	9.6397	9.6318	8.7465	9.6994	1.03e-01	3.62
20	960	9.6397	9.6396	9.3945	9.6623	2.81e-02	3.55
25	1 482	9.6397	9.6405	9.5958	9.6439	5.00e-03	3.47
30	3 222	9.6397	9.6399	9.6309	9.6407	1.02e-03	3.41
35	4 140	9.6397	9.6398	9.6354	9.6402	4.96e-04	3.38
40	7 212	9.6397	9.6398	9.6384	9.6399	1.58e-04	3.44
45	12 204	9.6397	9.6397	9.6392	9.6398	5.77e-05	3.53

Table 16: [Adaptive mesh refinement, L-shaped domain, discontinuous Galerkin method, $p = 2$] Lower and upper bounds of the exact eigenvalue λ_1, the relative eigenvalue error, and the eigenvector effectivity index; mixed accuracy auxiliary bounds $\underline{\lambda}_1 = \pi^2/2$ and $\underline{\lambda}_2 = 15.1753$

Note that the discriminant of this quadratic inequality is the term d_h and that it is non-negative. Thus

$$e_h \geq \frac{-(\underline{\lambda}_1 + 2l_h) + \sqrt{d_h}}{2}$$

and the desired bound follows. Note finally that for this estimate to actually improve on (6.15), $\tilde{\eta}_1$ needs to be positive, which follows when $\underline{\lambda}_1 R_h > l_h^2$ and $\|\nabla\tilde{s}_{1h}\|^2 < \underline{\lambda}_2$. □

References

[1] M. Ainsworth, *Robust a posteriori error estimation for nonconforming finite element approximation*, SIAM J. Numer. Anal., 42 (2005), pp. 2320–2341.

[2] ——, *A posteriori error estimation for discontinuous Galerkin finite element approximation*, SIAM J. Numer. Anal., 45 (2007), pp. 1777–1798.

[3] P. F. Antonietti, A. Buffa, and I. Perugia, *Discontinuous Galerkin approximation of the Laplace eigenproblem*, Comput. Methods Appl. Mech. Engrg., 195 (2006), pp. 3483–3503.

[4] P. F. Antonietti, P. Houston, and I. Smears, *A note on optimal spectral bounds for nonoverlapping domain decomposition preconditioners for hp-version discontinuous Galerkin methods*, Int. J. Numer. Anal. Model., 13 (2016), pp. 513–524.

[5] T. Arbogast and Z. Chen, *On the implementation of mixed methods as nonconforming methods for second-order elliptic problems*, Math. Comp., 64 (1995), pp. 943–972.

[6] M. G. Armentano and R. G. Durán, *Asymptotic lower bounds for eigenvalues by nonconforming finite element methods*, Electron. Trans. Numer. Anal., 17 (2004), pp. 93–101.

[7] D. N. Arnold and F. Brezzi, *Mixed and nonconforming finite element methods: implementation, postprocessing and error estimates*, RAIRO Modél. Math. Anal. Numér., 19 (1985), pp. 7–32.

[8] I. Babuška and J. Osborn, *Eigenvalue problems*, in Handbook of numerical analysis, Vol. II, Handb. Numer. Anal., II, North-Holland, Amsterdam, 1991, pp. 641–787.

[9] J. Blechta, J. Málek, and M. Vohralík, *Localization of the $W^{-1,q}$ norm for local a posteriori efficiency.* HAL Preprint 01332481, submitted for publication, 2016.

[10] D. Boffi, *Finite element approximation of eigenvalue problems*, Acta Numer., 19 (2010), pp. 1–120.

[11] D. Boffi, F. Brezzi, and L. Gastaldi, *On the problem of spurious eigenvalues in the approximation of linear elliptic problems in mixed form*, Math. Comp., 69 (2000), pp. 121–140.

[12] D. Braess, V. Pillwein, and J. Schöberl, *Equilibrated residual error estimates are p-robust*, Comput. Methods Appl. Mech. Engrg., 198 (2009), pp. 1189–1197.

[13] D. Braess and J. Schöberl, *Equilibrated residual error estimator for edge elements*, Math. Comp., 77 (2008), pp. 651–672.

[14] S. C. Brenner, *Poincaré-Friedrichs inequalities for piecewise H^1 functions*, SIAM J. Numer. Anal., 41 (2003), pp. 306–324.

[15] F. Brezzi and M. Fortin, *Mixed and hybrid finite element methods*, vol. 15 of Springer Series in Computational Mathematics, Springer-Verlag, New York, 1991.

[16] E. Cancès, G. Dusson, Y. Maday, B. Stamm, and M. Vohralík, *A perturbation-method-based a posteriori estimator for the planewave discretization of nonlinear Schrödinger equations*, C. R. Math. Acad. Sci. Paris, 352 (2014), pp. 941–946.

[17] E. Cancès, G. Dusson, Y. Maday, B. Stamm, and M. Vohralík, *Guaranteed and robust a posteriori bounds for Laplace eigenvalues and eigenvectors: conforming approximations*, SIAM J. Numer. Anal., 55 (2017), pp. 2228–2254.

[18] E. Cancès, G. Dusson, Y. Maday, B. Stamm, and M. Vohralík, *Guaranteed a posteriori bounds for eigenvalues and eigenvectors: multiplicities and clusters.* In preparation, 2018.

[19] C. Carstensen and S. A. Funken, *Fully reliable localized error control in the FEM*, SIAM J. Sci. Comput., 21 (1999/00), pp. 1465–1484.

[20] C. Carstensen and J. Gedicke, *Guaranteed lower bounds for eigenvalues*, Math. Comp., 83 (2014), pp. 2605–2629.

[21] C. Carstensen, J. Gedicke, and D. Rim, *Explicit error estimates for Courant, Crouzeix-Raviart and Raviart-Thomas finite element methods*, J. Comput. Math., 30 (2012), pp. 337–353.

[22] C. Carstensen and C. Merdon, *Computational survey on a posteriori error estimators for non-conforming finite element methods for the Poisson problem*, J. Comput. Appl. Math., 249 (2013), pp. 74–94.

[23] P. Ciarlet, Jr. and M. Vohralík, *Localization of global norms and robust a posteriori error control for transmission problems with sign-changing coefficients*, M2AN Math. Model. Numer. Anal., (2018). Accepted for publication.

[24] P. G. Ciarlet, *The Finite Element Method for Elliptic Problems*, vol. 4 of Studies in Mathematics and its Applications, North-Holland, Amsterdam, 1978.

[25] M. Costabel and A. McIntosh, *On Bogovskiĭ and regularized Poincaré integral operators for de Rham complexes on Lipschitz domains*, Math. Z., 265 (2010), pp. 297–320.

[26] E. A. Dari, R. G. Durán, and C. Padra, *A posteriori error estimates for non-conforming approximation of eigenvalue problems*, Appl. Numer. Math., 62 (2012), pp. 580–591.

[27] L. Demkowicz, J. Gopalakrishnan, and J. Schöberl, *Polynomial extension operators. Part I*, SIAM J. Numer. Anal., 46 (2008), pp. 3006–3031.

[28] ——, *Polynomial extension operators. Part III*, Math. Comp., 81 (2012), pp. 1289–1326.

[29] P. Destuynder and B. Métivet, *Explicit error bounds for a nonconforming finite element method*, SIAM J. Numer. Anal., 35 (1998), pp. 2099–2115.

[30] P. Destuynder and B. Métivet, *Explicit error bounds in a conforming finite element method*, Math. Comp., 68 (1999), pp. 1379–1396.

[31] D. A. Di Pietro and A. Ern, *Mathematical aspects of discontinuous Galerkin methods*, vol. 69 of Mathématiques & Applications (Berlin) [Mathematics & Applications], Springer, Heidelberg, 2012.

[32] V. Dolejší, A. Ern, and M. Vohralík, *hp-adaptation driven by polynomial-degree-robust a posteriori error estimates for elliptic problems*, SIAM J. Sci. Comput., 38 (2016), pp. A3220–A3246.

[33] W. Dörfler, *A convergent adaptive algorithm for Poisson's equation*, SIAM J. Numer. Anal., 33 (1996), pp. 1106–1124.

[34] R. G. Durán, L. Gastaldi, and C. Padra, *A posteriori error estimators for mixed approximations of eigenvalue problems*, Math. Models Methods Appl. Sci., 9 (1999), pp. 1165–1178.

[35] A. Ern, S. Nicaise, and M. Vohralík, *An accurate* $\mathbf{H}(\mathrm{div})$ *flux reconstruction for discontinuous Galerkin approximations of elliptic problems*, C. R. Math. Acad. Sci. Paris, 345 (2007), pp. 709–712.

[36] A. Ern and M. Vohralík, *A posteriori error estimation based on potential and flux reconstruction for the heat equation*, SIAM J. Numer. Anal., 48 (2010), pp. 198–223.

[37] ——, *Adaptive inexact Newton methods with a posteriori stopping criteria for nonlinear diffusion PDEs*, SIAM J. Sci. Comput., 35 (2013), pp. A1761–A1791.

[38] ——, *Polynomial-degree-robust a posteriori estimates in a unified setting for conforming, nonconforming, discontinuous Galerkin, and mixed discretizations*, SIAM J. Numer. Anal., 53 (2015), pp. 1058–1081.

[39] ——, *Stable broken* H^1 *and* $\boldsymbol{H}(\mathrm{div})$ *polynomial extensions for polynomial-degree-robust potential and flux reconstruction in three space dimensions*. HAL Preprint 01422204, submitted for publication, 2016.

[40] S. Giani and E. J. C. Hall, *An a posteriori error estimator for hp-adaptive discontinuous Galerkin methods for elliptic eigenvalue problems*, Math. Models Methods Appl. Sci., 22 (2012), pp. 1250030, 35.

[41] P. Grisvard, *Elliptic problems in nonsmooth domains*, vol. 24 of Monographs and Studies in Mathematics, Pitman (Advanced Publishing Program), Boston, MA, 1985.

[42] F. Hecht, *New development in FreeFem++*, J. Numer. Math., 20 (2012), pp. 251–265.

[43] F. Hecht, O. Pironneau, J. Morice, A. Le Hyaric, and K. Ohtsuka, *FreeFem++*, tech. report, Laboratoire Jacques-Louis Lions, Université Pierre et Marie Curie, Paris, http://www.freefem.org/ff++, 2012.

[44] B. Helffer, *Spectral theory and its applications*, vol. 139 of Cambridge Studies in Advanced Mathematics, Cambridge University Press, Cambridge, 2013.

[45] J. Hu, Y. Huang, and Q. Lin, *Lower bounds for eigenvalues of elliptic operators: by nonconforming finite element methods*, J. Sci. Comput., 61 (2014), pp. 196–221.

[46] J. Hu, Y. Huang, and Q. Shen, *The lower/upper bound property of approximate eigenvalues by nonconforming finite element methods for elliptic operators*, J. Sci. Comput., 58 (2014), pp. 574–591.

[47] S. Jia, H. Chen, and H. Xie, *A posteriori error estimator for eigenvalue problems by mixed finite element method*, Sci. China Math., 56 (2013), pp. 887–900.

[48] K.-Y. Kim, *A posteriori error analysis for locally conservative mixed methods*, Math. Comp., 76 (2007), pp. 43–66.

[49] ——, *A posteriori error estimators for locally conservative methods of nonlinear elliptic problems*, Appl. Numer. Math., 57 (2007), pp. 1065–1080.

[50] P. Ladevèze and D. Leguillon, *Error estimate procedure in the finite element method and applications*, SIAM J. Numer. Anal., 20 (1983), pp. 485–509.

[51] X. Liu, *A framework of verified eigenvalue bounds for self-adjoint differential operators*, Appl. Math. Comput., 267 (2015), pp. 341–355.

[52] X. Liu and F. Kikuchi, *Analysis and estimation of error constants for* P_0 *and* P_1 *interpolations over triangular finite elements*, J. Math. Sci. Univ. Tokyo, 17 (2010), pp. 27–78.

[53] F. Luo, Q. Lin, and H. Xie, *Computing the lower and upper bounds of Laplace eigenvalue problem: by combining conforming and nonconforming finite element methods*, Sci. China Math., 55 (2012), pp. 1069–1082.

[54] S. Mao and Z.-c. Shi, *Explicit error estimates for mixed and nonconforming finite elements*, J. Comput. Math., 27 (2009), pp. 425–440.

[55] V. Mehrmann and A. Miedlar, *Adaptive computation of smallest eigenvalues of self-adjoint elliptic partial differential equations*, Numer. Linear Algebra Appl., 18 (2011), pp. 387–409.

[56] B. Mercier, J. Osborn, J. Rappaz, and P.-A. Raviart, *Eigenvalue approximation by mixed and hybrid methods*, Math. Comp., 36 (1981), pp. 427–453.

[57] J. Papež, Z. Strakoš, and M. Vohralík, *Estimating and localizing the algebraic and total numerical errors using flux reconstructions*, Numer. Math., 138 (2018), pp. 681–721.

[58] W. Prager and J. L. Synge, *Approximations in elasticity based on the concept of function space*, Quart. Appl. Math., 5 (1947), pp. 241–269.

[59] J. E. Roberts and J.-M. Thomas, *Mixed and hybrid methods*, in Handbook of Numerical Analysis, Vol. II, North-Holland, Amsterdam, 1991, pp. 523–639.

[60] L. N. Trefethen and T. Betcke, *Computed eigenmodes of planar regions*, in Recent advances in differential equations and mathematical physics, vol. 412 of Contemp. Math., Amer. Math. Soc., Providence, RI, 2006, pp. 297–314.

[61] M. Vohralík, *On the discrete Poincaré–Friedrichs inequalities for nonconforming approximations of the Sobolev space H^1*, Numer. Funct. Anal. Optim., 26 (2005), pp. 925–952.

[62] ——, *A posteriori error estimates for lowest-order mixed finite element discretizations of convection-diffusion-reaction equations*, SIAM J. Numer. Anal., 45 (2007), pp. 1570–1599.

[63] Y. Yang, J. Han, H. Bi, and Y. Yu, *The lower/upper bound property of the Crouzeix–Raviart element eigenvalues on adaptive meshes*, J. Sci. Comput., 62 (2015), pp. 284–299.